

EXAMINING SHALLOW STRATIGRAPHIC, LITHOLOGIC,
AND WATER-SATURATION TRENDS AT THE WCS FACILITY,
ANDREWS COUNTY, TEXAS USING ELECTROMAGNETIC INDUCTION

by

Jeffrey G. Paine and Changbing Yang

Bureau of Economic Geology
John A. and Katherine G. Jackson School of Geosciences
The University of Texas at Austin
University Station, Box X
Austin, Texas 78713

Corresponding author
jeff.paine@beg.utexas.edu
(512) 471-1260
TBPG License No. 3776

Report prepared for
Texas Commission on Environmental Quality
Contract No. 582-4-69718

January 2010
Revised October 2010

CONTENTS

Introduction	1
Methods	4
Results	7
Frequency-Domain EM Data	8
EM Pseudosections	12
Line 1	12
Line 2	15
Line 3	17
Line 4	19
Line 5	21
Differing Triassic and Conductive-Zone Depths	23
Conclusions	25
Acknowledgments	26
References	27
Appendix A: Data Points and Borings along Conductivity Pseudosections	29
Appendix B: Time-Domain Electromagnetic Induction Soundings	34

FIGURES

1. Aerial photographic map of the WCS facility, Andrews County, Texas	1
2. Borings with reported depths to Triassic redbed strata and wells with reported OAG water	3
3. Location of geophysical profiles and time-domain electromagnetic soundings	4
4. Approximate exploration depth of various coil separations and coil orientations of the Geonics EM34-3 ground conductivity meter.	5
5. (a) Generalized time-domain EM transmitter loop current and receiver loop response, and (b) Field layout for terraTEM time-domain soundings	6
6. Apparent ground conductivity along lines 1 through 5 measured with the Geonics EM34 at a coil separation of 20 m	9

7. Apparent ground conductivity along lines 1 through 5 measured with the Geonics EM34 at a coil separation of 40 m	10
8. Apparent conductivity pseudosection and supporting data along EM line 1.	13
9. Apparent conductivity pseudosection and supporting data along EM line 2.	16
10. Apparent conductivity pseudosection and supporting data along EM line 3.	18
11. Apparent conductivity pseudosection and supporting data along EM line 4.	20
12. Apparent conductivity pseudosection and supporting data along EM line 5.	22
13. Difference areas along EM lines where estimated depths to the electrically conductive layer are significantly deeper than interpreted depths to Triassic redbed strata	24
A1. Data points, noise sources, and names of wells and borings along EM line 1	29
A2. Data points, noise sources, and names of wells and borings along EM line 2	30
A3. Data points, noise sources, and names of wells and borings along EM line 3	31
A4. Data points, noise sources, and names of wells and borings along EM line 4	32
A5. Data points, noise sources, and names of wells and borings along EM line 5	33

TABLES

1. Line orientation, line length, and acquisition dates for apparent conductivity data collected using the Geonics EM34 at the WCS site	5
2. Statistical summary of all apparent conductivity measurements at the WCS site using the Geonics EM34-3 ground conductivity meter.	7

INTRODUCTION

At least two important issues related to long-term waste disposal site proposed and operated by Waste Control Specialists, Inc. (WCS) in Andrews County, Texas (fig. 1) are related to shallow hydrostratigraphy. These are (a) depth to the clay-rich Triassic Dockum Group that hosts the waste repositories, and (b) subsurface distribution of water within the younger strata (Ogallala-Antlers-Gatuna units, or OAG) above the Dockum Group. Since the early 1990s, more than 400 borings and wells have been drilled by WCS that have helped understand the three-dimensional geologic and hydrologic environment at the WCS site. Nevertheless, uncertainty remains in the understanding of lithologic and hydrologic parameter distribution at and near the repository.

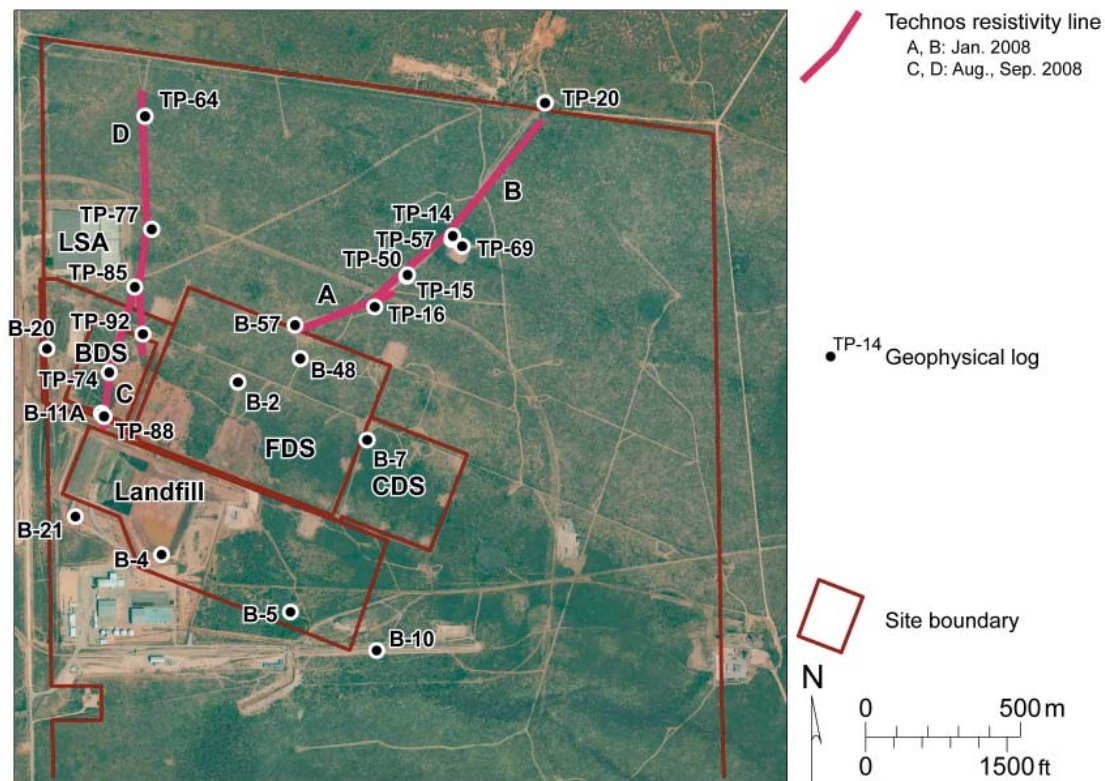


Figure 1. Aerial photographic map of the WCS facility, Andrews County, Texas showing the locations of resistivity lines acquired by Technos in 2008 (lines A through D) and boreholes for which geophysical logs (natural gamma and electrical conductivity) exist. Site and facility boundaries are approximate. Aerial image is a 2008 digital orthophotograph from the U.S. Department of Agriculture's National Agricultural Inventory Project acquired from the Texas Natural Resources Information System. LSA = Low Specific Activity storage pad; BDS = Byproduct Disposal Area; FDS = Federal Disposal Site; CDS = Compact Disposal Site.

Geophysical surveys that measure the electrical conductivity of the subsurface can be applied to help illuminate shallow hydrogeologic issues. At the WCS site, the generally higher clay content characteristic of the Triassic sediments has been shown through borehole geophysical measurements (Technos, 2008a, b) to cause a significant increase in electrical conductivity. Similarly, water saturation within the Ogallala-Antlers-Gatuna (OAG) strata is also associated with an increase in conductivity over lithologically similar strata that are dry (Technos, 2008a, b). Consequently, surface or subsurface geophysical surveys have the potential to augment site-specific borehole data to better define the subsurface distribution of lithologic materials and water.

Technos (2008a, b) conducted two surface resistivity surveys and accompanying natural gamma ray and electrical conductivity measurements in 15 boreholes across the WCS site (fig. 1). Borehole measurements demonstrated that dry OAG strata at the WCS site are poorly conductive, water-saturated OAG strata have intermediate conductivity, and clay-rich Triassic Dockum Group “redbeds” have the highest conductivities. Inverted resistivity-depth sections included in the Technos reports showed generally poor agreement between depth to a conductive layer and known depths to presumably conductive Triassic strata and no discernible relationship to OAG water saturation (Technos 2008a, b, and c). Nevertheless, borehole conductivity logs and uninverted plots of apparent resistivity at long electrode spacings from raw survey data provided by Technos suggest that there may be a correlation between apparent resistivity and water saturation (Paine, 2009) at the deepest exploration depths investigated in the resistivity survey. The inability of the inversions to accurately portray the depths to conductive Triassic bedrock is likely due to the limited exploration depth achieved by the resistivity survey (Paine, 2009).

Based on analyses of surface resistivity and borehole geophysical measurements acquired by Technos (2008a, b), researchers from the Bureau of Economic Geology (Bureau) acquired additional electrical conductivity data at the WCS site using the electromagnetic induction (EM) method (Parasnis, 1986; Frischknecht and others, 1991; West and Macnae, 1991) in an attempt

to better define depth to Triassic bedrock and determine whether EM data could help delineate subsurface moisture distribution within the OAG.

WCS borings and monitoring wells help constrain the thickness and character of OAG strata, the depth to the interpreted top of the Triassic Dockum Group (“redbeds”), and the presence or absence of water within lower OAG strata at the Triassic contact (fig. 2). Gridded depths to the top of WCS-interpreted Triassic strata range from a few meters to more than 30 m across the site (fig. 2). One of the prominent subsurface features is the “redbed ridge,” an interpreted local high on the Triassic surface that extends northwest-southeast across the southern part of the FDS and CDS and the northern part of the landfill area. Wells with water-saturated basal OAG strata (as of the May 2009 sampling event) are found northeast of the FDS and CDS, along the eastern site boundary, east of the CDS and landfill areas, and west of the FDS (fig. 2). EM lines and sound-

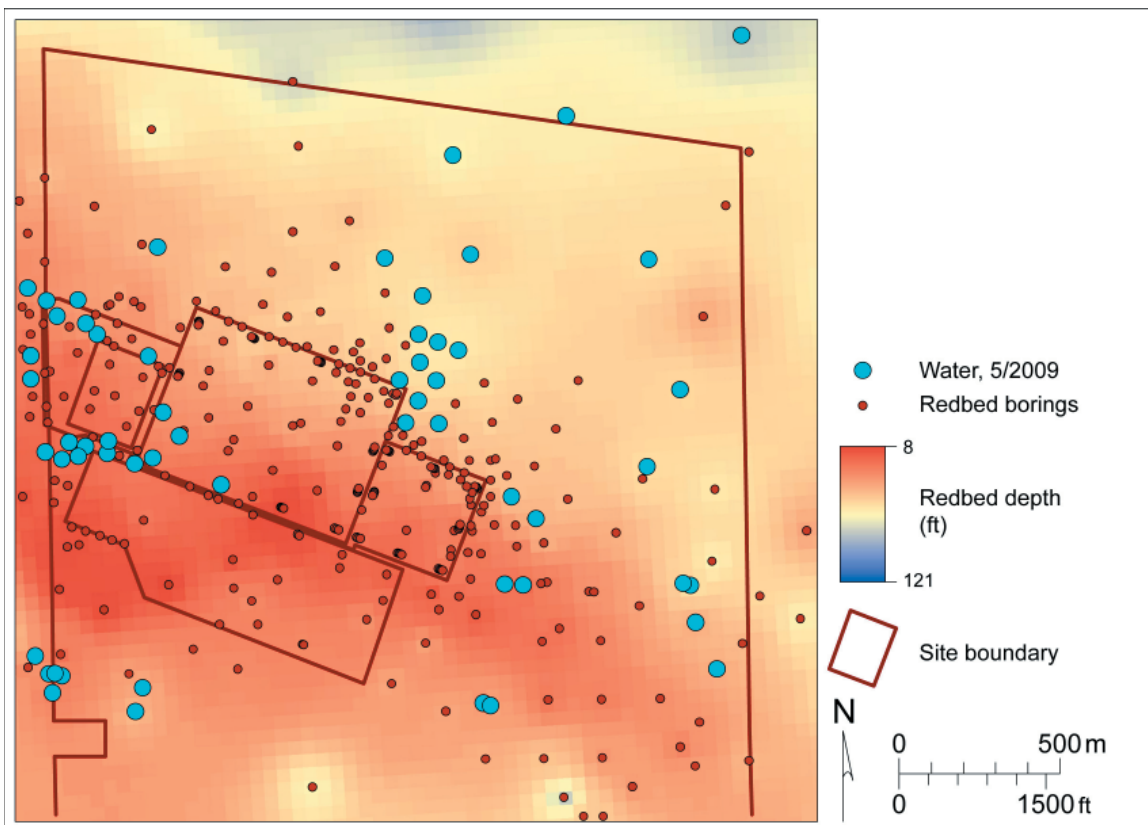


Figure 2. Borings with reported depths to Triassic redbed strata (red circles) and wells with reported OAG water in May 2009 superimposed on gridded depth to redbeds. Well and boring data provided by WCS to TCEQ.

ings were positioned to examine OAG lithologic and thickness variations and possible OAG water saturation trends across the site.

METHODS

Two types of EM surveys were conducted at the WCS in late June, early July, and November 2009. Frequency-domain EM surveys, in which a Geonics EM34-3 instrument was used to measure the apparent electrical conductivity of the ground to depths of 20 to 30 m, were conducted along five lines (two north-south and three east-west) across key areas of the WCS site (fig. 3 and table 1). This instrument employs two small electromagnetic coils (a transmitter and receiver coil) that can be separated by 10, 20, or 40 m depending on the exploration depth desired (fig. 4). At the WCS site, we operated the instrument at the 20- and 40-m separations to maximize pro-

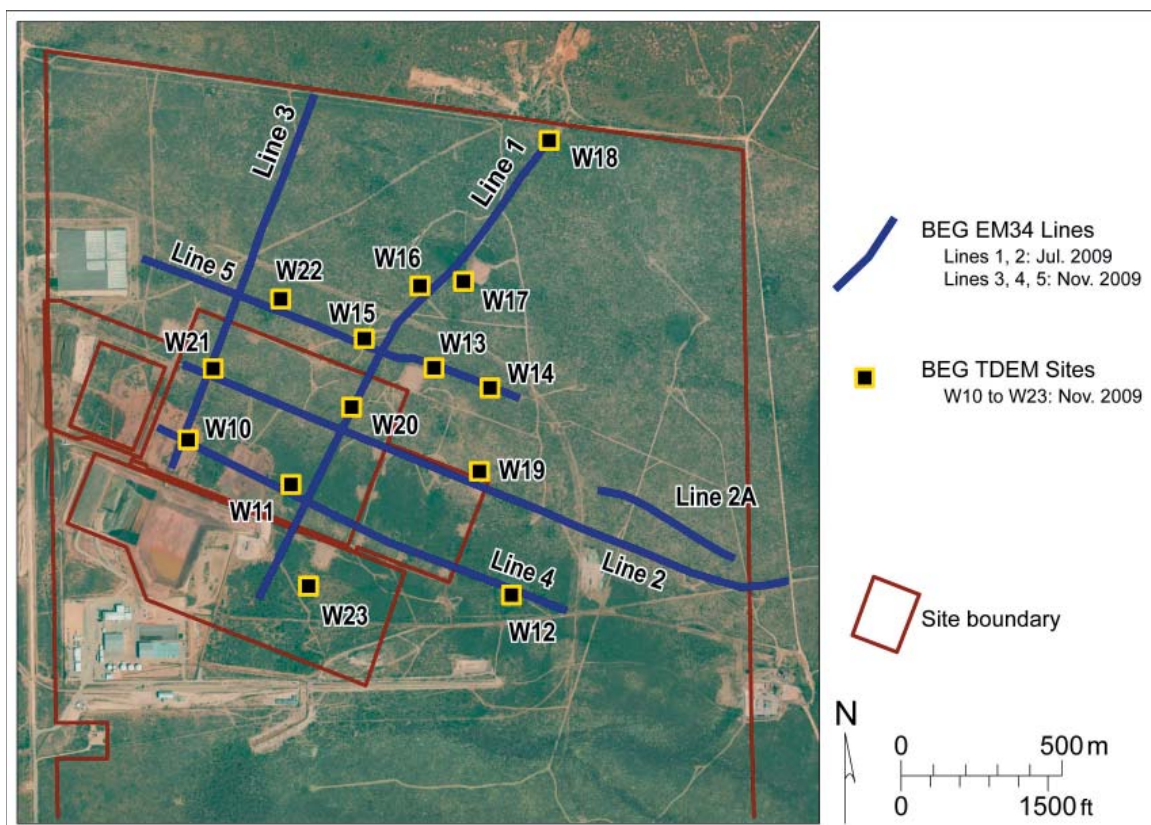


Figure 3. Location of geophysical profiles acquired in June, July, and November 2009 using a Geonics EM34 ground conductivity meter (lines 1 through 5) and time-domain electromagnetic soundings acquired using a Monex Geoscope terraTEM system (sites W10 through W23).

Table 1. Line orientation, line length, and acquisition dates for apparent conductivity data collected using the Geonics EM34 at the WCS site. Line locations are shown on fig. 3.

Line	Orientation	Length (m)	Dates acquired
1	SW-NE	1800	June 30 and July 1, 2009
2	NW-SE	2030	June 30 to July 2, 2009
3	SW-NE	1250	November 10, 2009
4	NW-SE	1400	November 11, 2009
5	NW-SE	1265	November 10, 2009

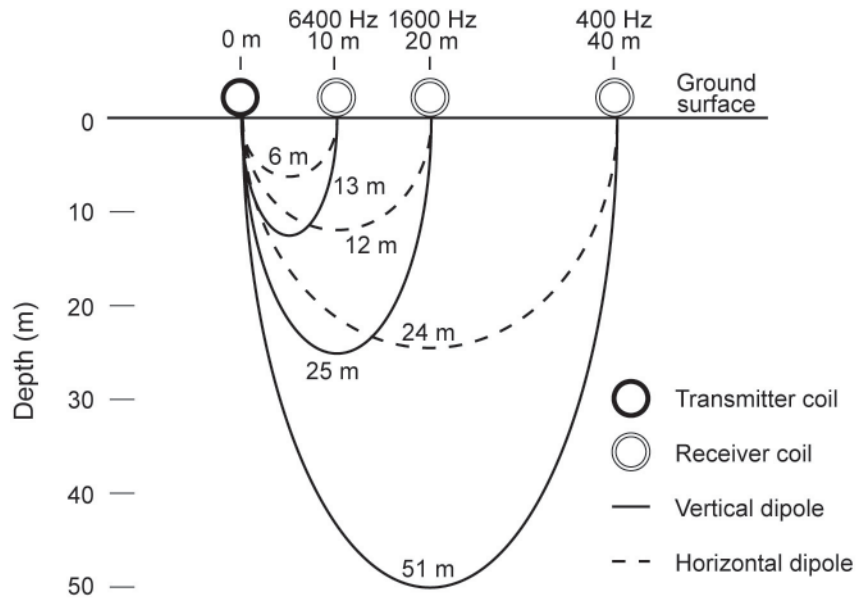


Figure 4. Approximate exploration depth of various coil separations and coil orientations of the Geonics EM34-3 ground conductivity meter (modified from McNeil, 1980).

ductivity, exploration depth, and the likelihood of sensing water saturation at the base of the OAG and underlying clay-rich bedrock strata.

Frequency-domain EM data are displayed as apparent conductivity at two coil separations (20 and 40 m) and two coil orientations (vertical dipole and horizontal dipole) for each separation. Approximate exploration depths for these configurations range from about 12 to about 50 m (fig. 4). These four measurements have also been combined to produce apparent conductiv-

ity pseudosections by assigning an approximate plotting depth for each configuration and then gridding all measurements at all configurations along a line. Assigned depths for the four coil configurations are, from shallowest to deepest, 8 m for the 20 m horizontal dipole (HD) separation, 12 m for the 20 m vertical dipole (VD) separation, 16 m for the 40 m HD separation, and 24 m for the 40 m VD separation.

Four apparent conductivity measurements at a given location can also be used to produce a simple two-layer conductivity model using the inversion software IX1D by Interpex. These one-dimensional inversions were completed at selected sites along lines 1 and 2 to verify the assigned plotting depths for the continuous EM pseudosections that are better for visualizing vertical and lateral differences that could be related to changes in hydrologic and lithologic conditions.

In November, we deployed a new time-domain EM (TDEM) instrument, the terraTEM system manufactured by Monex Geoscope, to the WCS site in an attempt to explore deeper at selected sites than possible with the Geonics EM34. The terraTEM soundings were acquired at 14 loca-

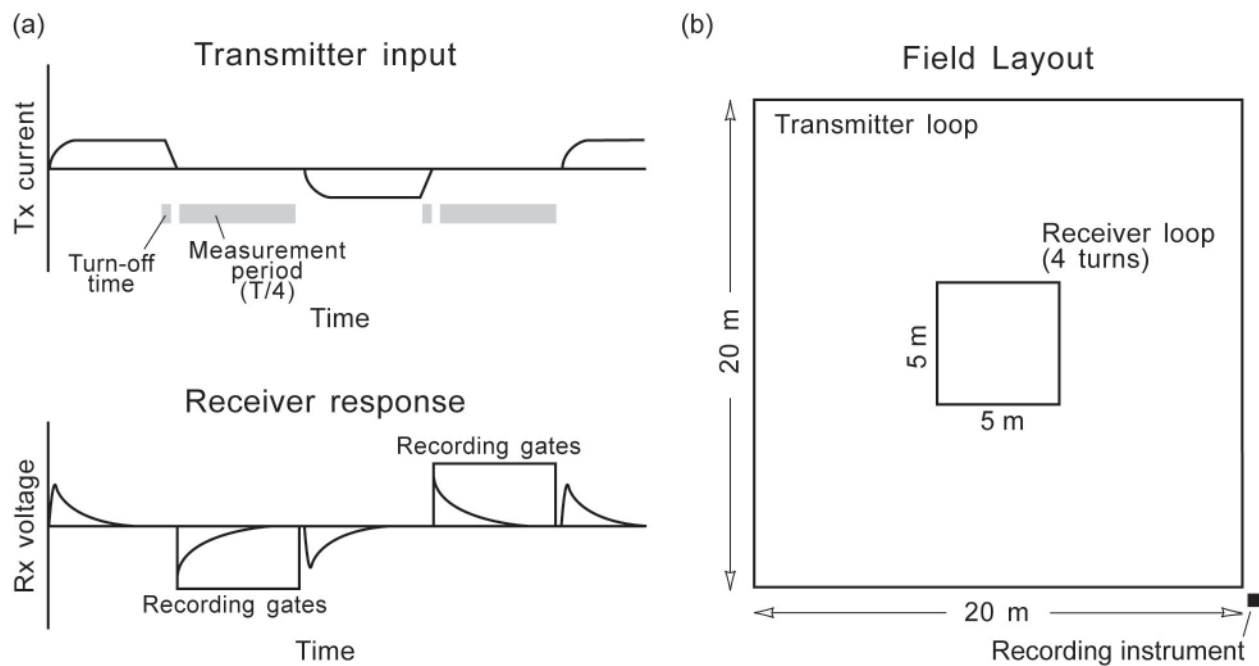


Figure 5. (a) Generalized time-domain EM transmitter loop current (top) and receiver loop response (bottom). (b) Field layout employed for terraTEM time-domain soundings at the WCS site.

tions (fig. 3) to complement the five EM34 lines. For these soundings, we set up a 20×20 m, single-wire loop to serve as a transmitter, through which we circulated 3 to 4 amperes constant electric current (fig. 5). This current creates a magnetic field that collapses when the current is shut off over a short time (typically a few microseconds). The collapsing primary magnetic field induces electrical currents in the subsurface, which generate a secondary magnetic field as the currents propagate downward and outward. We used a 4-turn, 5×5 m receiver loop at the center of the transmitter loop to measure the decay of the magnetic field generated by these secondary ground currents. The measured magnitude and rate of decay of this secondary magnetic field (over a millisecond or two after transmitter turnoff) is influenced by the subsurface conductivity structure. We used the software IX1D by Interpex to construct subsurface conductivity models to fit the decays observed at the 14 TDEM sites.

RESULTS

Geophysical data acquired using the frequency- and time-domain EM systems were of generally good quality except near noise sources such as power lines and large metallic objects such as train cars. Frequency-domain EM data demonstrated that electrical conductivities within the exploration depth range of the instrument generally increase with depth (table 2). Relatively coarse-grained and dry OAG strata are poorly conductive; finer-grained (clay-rich) Triassic strata are more conductive. These general observations, as well as the apparent conductivities, are

Table 2. Statistical summary of all apparent conductivity measurements at the WCS site using the Geonics EM34-3 ground conductivity meter at the 20- and 40-m coil separation and the horizontal dipole (HD) and vertical dipole (VD) coil orientation.

Coil separation (m)	Orientation	n	Mean (mS/m)	Minimum (mS/m)	Maximum (mS/m)	Std. dev. (mS/m)
20	HD	382	21.4	10	43	5.0
20	VD	379	25.8	5	47	6.0
40	HD	327	35.8	26	58	6.2
40	VD	311	38.9	28	75	6.0

reasonably consistent with subsurface data from borehole conductivity logs acquired by Technos (2008a, b). Both EM instruments appear to have explored into Triassic strata across most of the site. The frequency-domain system (Geonics EM34) may not have reached Triassic bedrock over the deepest bedrock areas at the north side of the site.

Frequency-Domain EM Data

One way to present the frequency-domain conductivity data acquired with the Geonics EM34 is to show actual apparent conductivity measurements at each successively deeper-exploring coil separation and configuration (fig. 4) and examine the magnitude and change in those measurements across the site to look for possible relationships among stratigraphic, lithologic, and hydrologic causes of change.

The lowest apparent conductivities measured with the EM34 were at the 20-m separation and horizontal-dipole (HD) orientation (table 2 and fig. 6a), which achieves the shallowest exploration depth measured at the WCS site and the one most likely to respond to at- and very near-surface variations in clay and water content. These data show relatively little lateral variation along lines 1 through 5 across the site. Apparent conductivities at the upper end of the observed 10 to 43 mS/m range are located (1) at the southwestern part of the FDS at the southern end of line 3 and the western ends of lines 2 and 4, (2) across part of the landfill area at the southern end of line 1, and (3) at the northern edge of the CDS along line 2. Elevated shallow values are also located near the small playa at the east end of line 4.

The apparent conductivities generally increase across the site for the measurements made with the same 20-m coil separation and the deeper-exploring, vertical-dipole (VD) orientation (table 2 and fig. 6b). Areas of relatively high apparent conductivities that might indicate increased moisture or clay content within the exploration depth are similar to those identified in the 20-m HD measurements. There is an additional area of elevated conductivity east of the LSA pad at the west end of line 5. As was true for the 20-m HD data, elevated shallow apparent conductivities

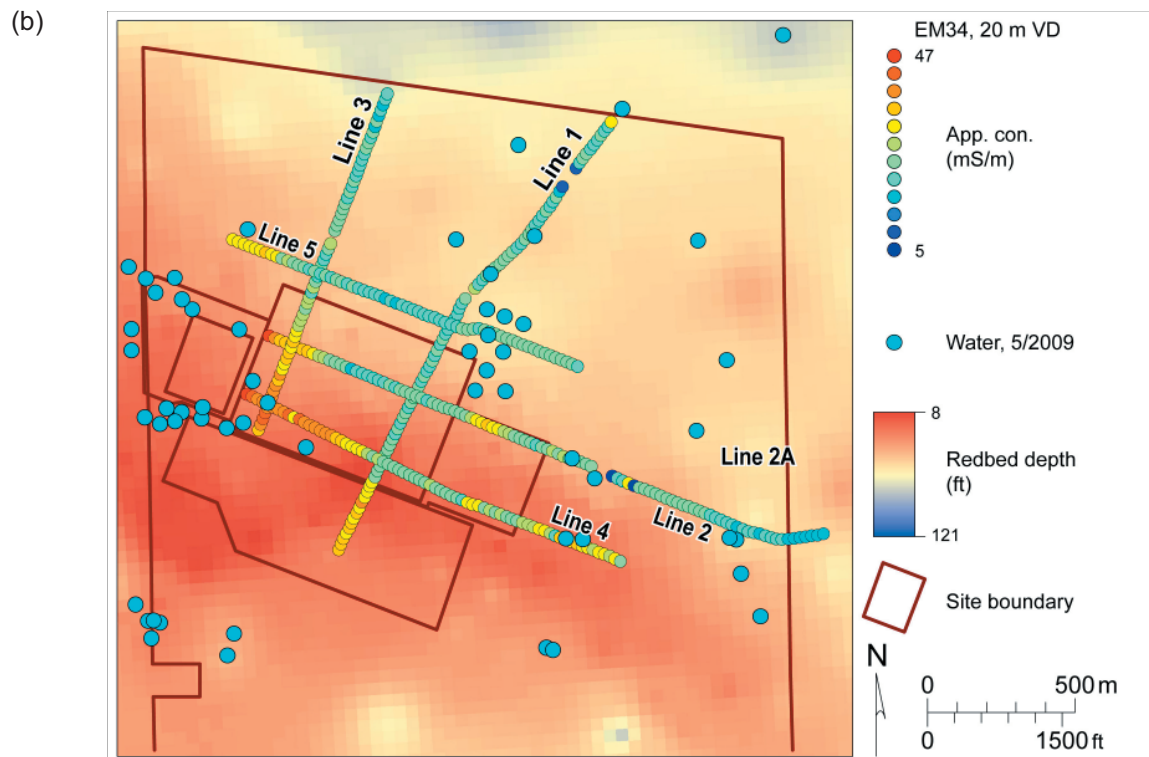
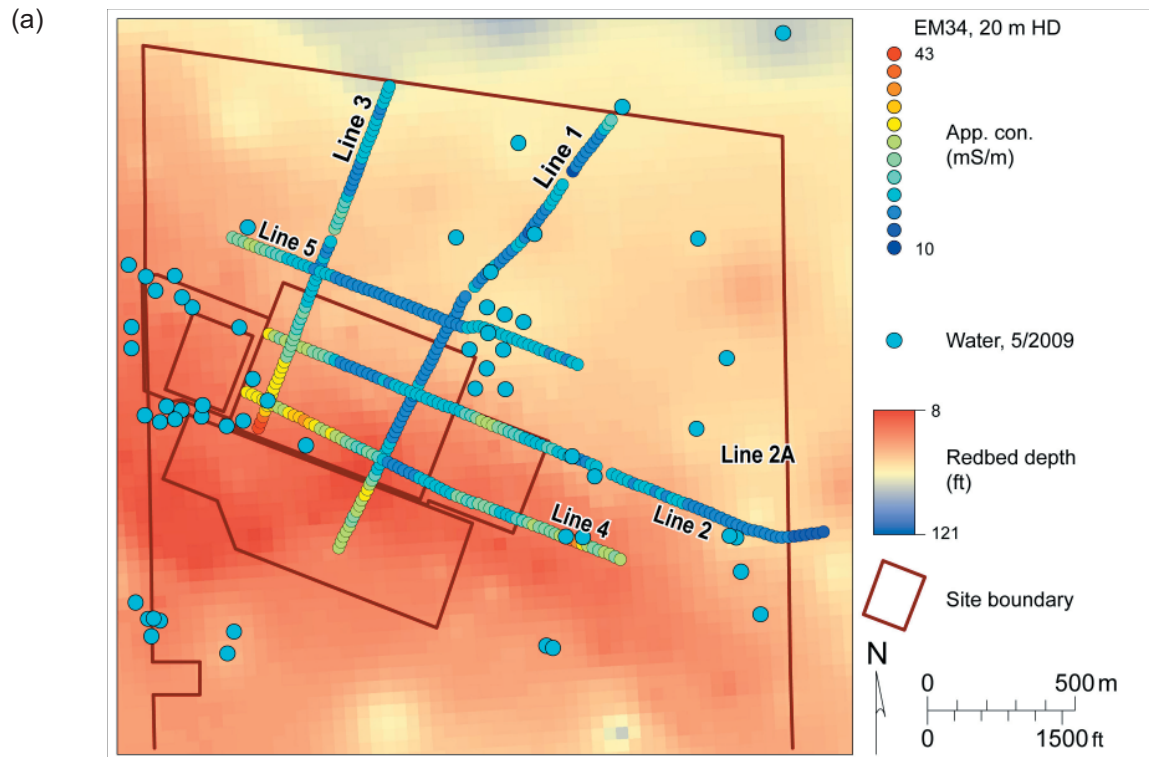


Figure 6. Apparent ground conductivity along lines 1 through 5 measured with the Geonics EM34 at a coil separation of 20 m and the (a) horizontal dipole (HD) and (b) vertical dipole (VD) coil orientation. Data are superimposed on the gridded depth-to-redbed surface and the locations of wells with reported OAG water in May 2009.

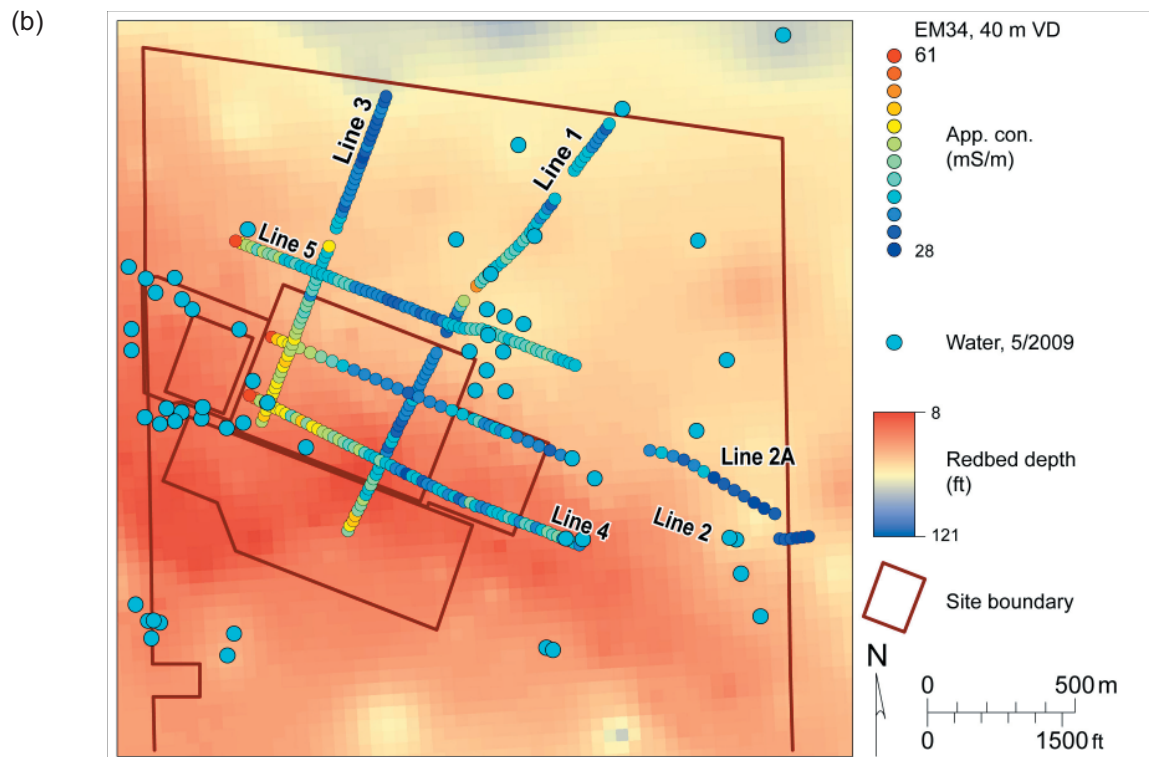
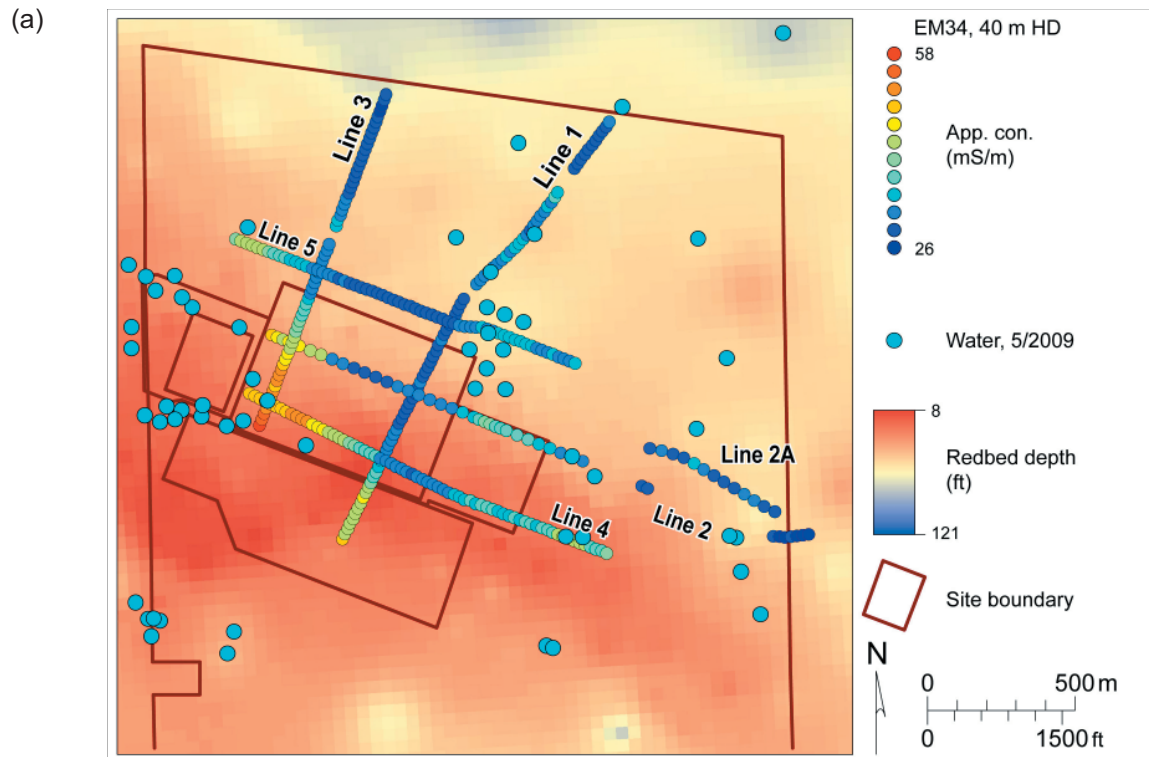


Figure 7. Apparent ground conductivity along lines 1 through 5 measured with the Geonics EM34 at a coil separation of 40 m and the (a) horizontal dipole (HD) and (b) vertical dipole (VD) coil orientation. Data are superimposed on the gridded depth-to-redbed surface and the locations of wells with reported OAG water in May 2009.

are observed near the small playa at the east end of line 4, but not at the larger playa north of the FDS on line 1.

Further general increase in apparent conductivity is evident in the data acquired at 40-m separation and HD coil orientation (table 2 and fig. 7a). Highest conductivities are again found in the southwest part of the FDS at the western end of lines 2 and 4 and the southern end of line 3, where borehole data suggest that the depth to the Triassic redbed surface shallows. Borehole data indicate that the depth to the redbed surface remains relatively shallow along the crest of the “redbed ridge” trending southeastward beneath line 4, but apparent conductivity is lower along the middle section of this line. This observation suggests that either the redbed surface dips below the exploration depth of this configuration (contrary to borehole data) or that the lithology at that depth range changes to a coarser, lower clay content material.

Elevated conductivities near the LSA pad at the west end of line 5 may be a response to a similar shallowing of Triassic clay-rich strata or an increase in basal OAG moisture content. Elevated conductivities are also observed along the northern edge of the CDS, near a cluster of wells near the northeast corner of the FDS, and near the small playa east of the CDS on line 4. The coincidence of these areas of elevated conductivity with known OAG water saturation suggests that elevated moisture content may be the prime cause of the increased apparent conductivity at these sites.

Similar trends are observed in the deepest exploring, 40-m VD coil configuration (table 2 and fig. 7b). Apparent conductivities are the highest observed at the site, likely reflecting an exploration depth sufficient to more fully sense the clay-rich Triassic strata and basal OAG saturated zones. Low apparent conductivities at the northern ends of lines 1 and 3 suggest that relatively deep, clay-rich Triassic strata are beyond the exploration depth of this instrument in these areas. Elevated conductivities occur again at the southwestern part of the FDS, east of the LSA pad, and near the cluster of water wells reporting saturated OAG strata northeast of the FDS on lines 1 and 5. Decreasing apparent conductivities eastward along the postulated “redbed ridge” beneath

line 4 again suggest either an unrecognized deepening of the clay-rich Triassic contact or a lateral coarsening of strata along the ridge.

EM Pseudosections

Pseudosections displaying gridded apparent conductivity plotted at assigned depths have been constructed for lines 1 through 5 from the four measurements at 10- and 20-m coil separation and horizontal and vertical dipole coil orientations. These images do not display inverted, “true” conductivity and depth relationships, but are useful in examining lateral and vertical conductivity trends along the lines. Comparisons with borehole-based Triassic depths, two-layer inversions of EM34 data at select locations, and inversions of time-domain EM data all suggest that the depth relationships depicted on the pseudosections reasonably reflect true subsurface relationships. Pseudosections have the interpretational advantage of not introducing inversion artifacts into a relatively laterally homogeneous shallow subsurface. Locations of apparent conductivity measurements used to create the gridded pseudosections, along with the locations, names, and distances from the lines for the nearest boreholes and wells, are in Appendix A.

Line 1

Line 1 extends 1800 m to the northeast from the middle part of the proposed RCRA landfill extension, across the eastern part of the FDS, across a playa north of the FDS, and ends at the northern site boundary (fig. 3 and table 1). Ground-surface elevation generally rises to the northeast along this line, but there is a local low at the playa (fig. 8). Elevations at the top of the Triassic redbeds, interpreted by WCS from borehole data, depict a notable thinning of the OAG between the southern end of the line and the northern boundary of the FDS (the “redbed ridge” that underlies much of the FDS and CDS). Depths to the top of the Triassic increase to the north as the land surface rises. Data from 15 boreholes (fig. A1, Appendix A) at distances of 3 to 58 m from line 1 provide the stratigraphic control for this line. OAG saturated thicknesses of 1.5 to 2.1 m were reported for playa-area wells TP-14 and TP-15; all other borings along this line have

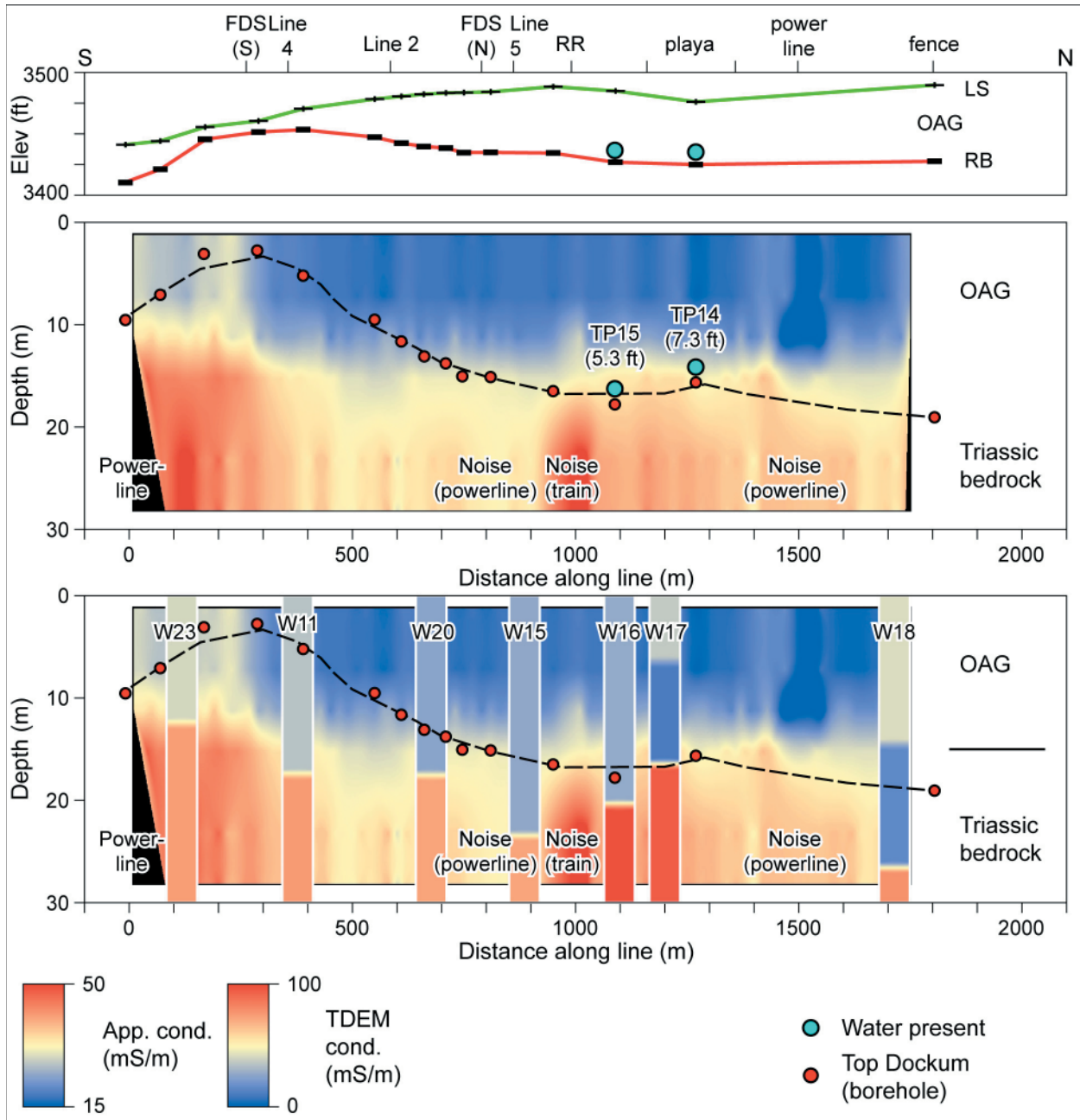


Figure 8. Apparent conductivity pseudosection and supporting data along EM line 1 (fig. 3). (top) Elevation of land-surface (LS) and the top of Triassic redbed surface (RB) and location of wells with OAG water in May 2009. (middle) Gridded apparent conductivity measurements made using the Geonics EM34-3. Also shown are nearby borehole-based depths to the top of the Triassic, OAG saturated thickness in May 2009, and Triassic depths interpolated from borehole data (dashed line), and noise sources and locations. (bottom) Best-fit conductivity models from time-domain EM soundings (fig. 3; Appendix B) near EM line 1 superimposed on the conductivity pseudosection. Surface elevation from USGS topographic maps and surface elevations, stratigraphic interpretations, contact depths, and water data provided to TCEQ by WCS.

been reported to be dry within the OAG. Sources of EM noise, and consequently lower confidence in the data, include power lines at distances of 0, 800, and 1500 m along the line and a train and railroad tracks at about 1000 m (fig. 8).

The line 1 pseudosection reveals the limited lateral variability in apparent conductivity and the pronounced increase in apparent conductivity with depth (fig. 8). Comparisons with available borehole data show that, for the southern end and the northern half of the line, a pronounced increase in apparent conductivity coincides with the borehole-based interpretation of Triassic bedrock. Above this, the generally low apparent conductivity correlates with relatively coarse-grained OAG strata. The only location where the depth to the conductive zone is shallower than the depth to Triassic bedrock is near the playa north of the FDS, where saturated thicknesses in basal OAG strata are greater than 1 m. Borehole conductivity logs (Technos 2008a, b) indicate that basal OAG water saturation is accompanied by an increase in conductivity that could be the cause of conductive-zone shallowing.

Elevated apparent conductivity shallower than about 10 m at the southern 300 m of line 1 coincides with an area of dense vegetation and evidence of a relatively moist ground surface that may delineate an area of higher near-surface moisture content and a potential recharge area. This is part of a larger area of poor agreement between depths to the conductive layer and the borehole-based depth to the Triassic redbeds. The zone of poor agreement (the conductive layer is significantly deeper than the depth to the top of the Triassic) extends over most of the area of the “redbed ridge” between about 100 and 600 m along line 1. The cause of this depth discrepancy is likely either that the redbed ridge is composed mostly of coarser (non-clay) sediments than underlying, clay-rich strata, or that the top of the Triassic has been picked much shallower than the true depth. Boring descriptions in this area are similar to descriptions of Triassic strata in other boreholes, suggesting that the redbed ridge may indeed be Triassic but is likely to be composed of coarser sediment.

In addition to two-layer inversions of EM34 data at approximately 100-m intervals along the line, depths to the conductive layer were also compared to conductivity-depth profiles obtained from seven time-domain EM soundings acquired near line 1 (figs. 2 and 8; Appendix B). Three- and four-layer models for most of these soundings depict similar depths to the basal conductive layer to those shown on the pseudosection.

Line 2

Line 2 trends southeasterly for a distance of 2030 m from the western boundary of the FDS, along the northern boundary of the CDS, and ends near the eastern boundary of the site (fig. 3 and table 1). Surface elevations (fig. 9) reveal a broad, shallow topographic low across the eastern two-thirds of the line. Subsurface control on OAG thickness and depth to Triassic strata is provided by 20 borings and wells located 4 to 47 m from the line (borehole names and distances from the line are shown on fig. A2, Appendix A). Noise sources that locally degrade EM data quality are located at the western end of the line and between about 1200 and 1300 m along the line, just west of the railroad tracks. Power-line noise at the 40-m coil spacing required a northerly offset for those measurements east of the railroad tracks (line 2A, figs. 3 and 7).

The apparent conductivity pseudosection was gridded from all 20- and 40-m apparent conductivity measurements in non-noisy areas (contributing data points are shown on fig. A2, Appendix A). The section depicts generally low apparent conductivity in the upper 10 to 15 m underlain by higher-conductivity strata. Stratigraphic picks on the Triassic redbed surface correlate reasonably well with the upper boundary of the conductive zone, confirming that the low-conductivity section represents relatively coarse-grained and dry OAG strata and the underlying conductive zone represents relatively clay-rich Triassic Dockum strata. OAG strata are poorly conductive across the section except near the western end (0 to 200 m) and between 750 and 850 m along the line. The shallow increase at the west end may be influenced by shallowing, conductive Triassic strata or by elevated near-surface moisture content, although nearby borings are reported to

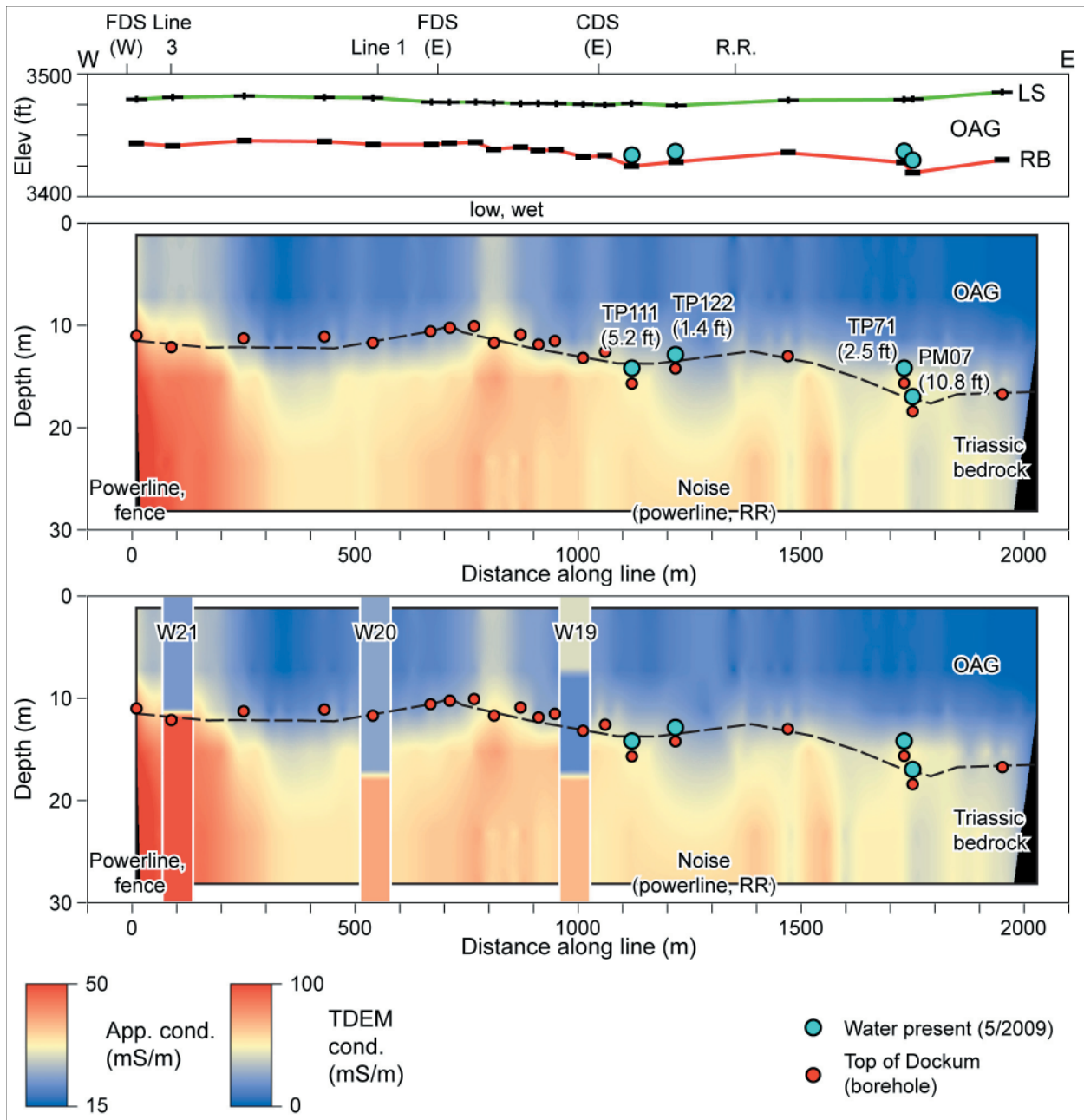


Figure 9. Apparent conductivity pseudosection and supporting data along EM line 2 (fig. 3). (top) Elevation of land-surface (LS) and the top of Triassic redbed surface (RB) and location of wells with OAG water in May 2009. (middle) Gridded apparent conductivity measurements made using the Geonics EM34-3. Also shown are nearby borehole-based depths to the top of the Triassic, OAG saturated thickness in May 2009, and Triassic depths interpolated from borehole data (dashed line), and noise sources and locations. (bottom) Best-fit conductivity models from time-domain EM soundings (fig. 3; Appendix B) near EM line 2 superimposed on the conductivity pseudosection. Surface elevation from USGS topographic maps and surface elevations, stratigraphic interpretations, contact depths, and water data provided to TCEQ by WCS.

be dry. The increase along the northern boundary of the CDS coincides with a local topographic low where field observations indicated elevated near-surface moisture content.

There is a local low in the basal conductive zone beneath the FDS between about 250 and 750 m along the line that is not evident from the borehole data, which show shallower Triassic depths in this area. A time-domain EM sounding (W20) in the center of this area (figs. 3 and 9; Appendix B) also shows depths to the conductive zone 4 to 5 m deeper than the borehole-based depth to the top of Triassic strata. This discrepancy between geophysical and borehole data suggests a lithologic change in Triassic strata that is characterized by coarser sediment and a reduction in clay content in this area.

Basal OAG saturated thicknesses of 0.5 m or more were reported for four wells along this line in the May 2009 sampling (fig. 9). Two of these wells (TP-111 and TP-122) are located in an area of EM noise where 40-m data quality is reduced, and two are near the eastern site boundary where Triassic bedrock deepens and the 20- and 40-m data are not coincident.

Line 3

Line 3 extends 1250 m northeasterly from the landfill area, along the western boundary of the FDS, and across the area north of the FDS to end at the northern site boundary (fig. 3 and table 1). Ground surface and stratigraphic data from WCS boreholes show that the OAG strata thicken northward along this line from less than 10 m at the southern end to more than 20 m at the northern end (fig. 10). Ground-surface elevation rises to the north, whereas the interpreted elevation at the top of Triassic strata decreases to the north. There are 14 boreholes and wells that are 0 to 95 m from the line (fig. A3, Appendix A). Only two (FWF-1A and TP-72 on the south end) have reported water saturation in basal OAG strata in the May 2009 sampling.

Sources of EM noise include power lines at the south end, near the northern boundary of the FDS at about 500 m along the line, and at the northern site boundary at the north end of the line

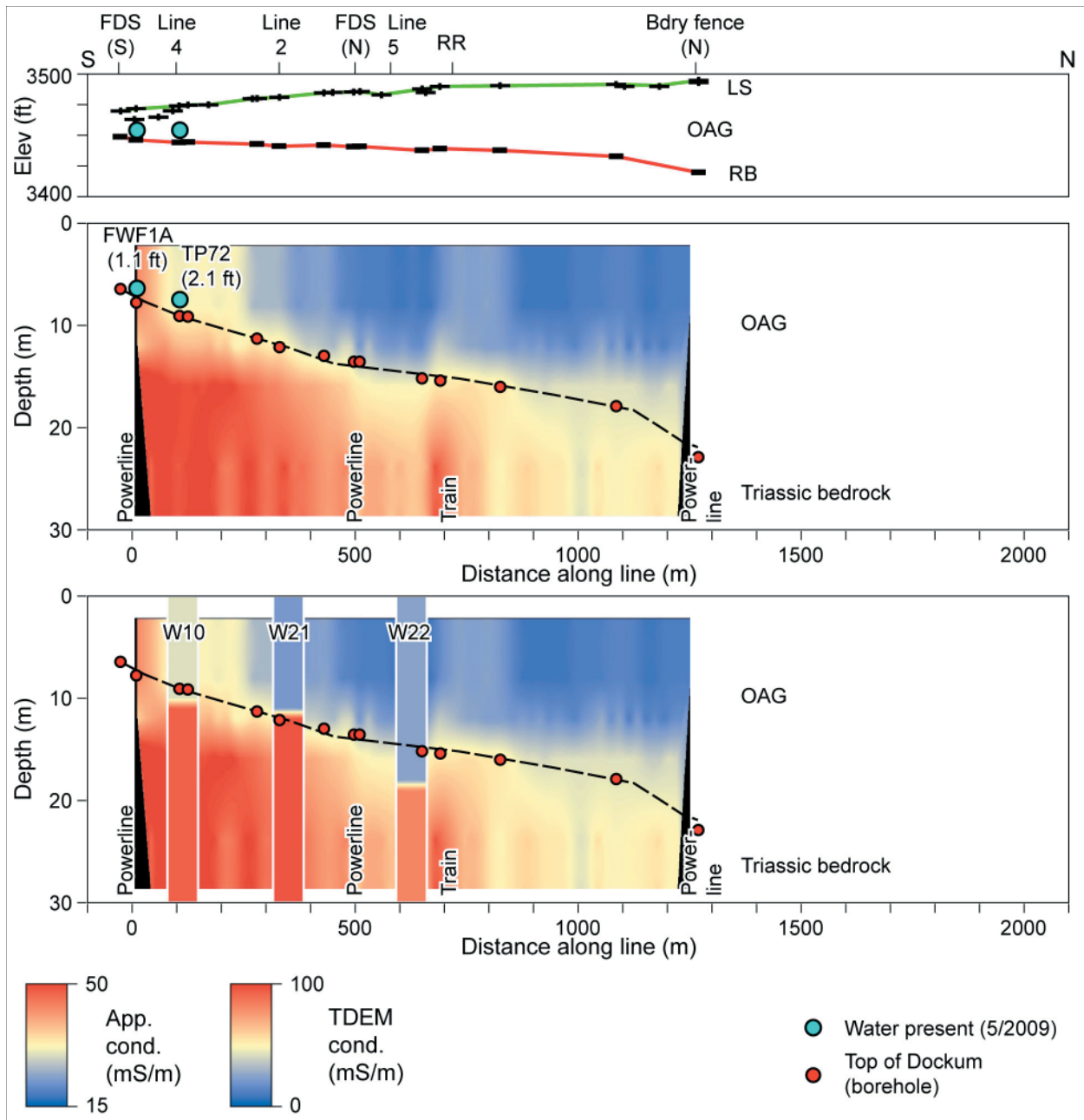


Figure 10. Apparent conductivity pseudosection and supporting data along EM line 3 (fig. 3). (top) Elevation of land-surface (LS) and the top of Triassic redbed surface (RB) and location of wells with OAG water in May 2009. (middle) Gridded apparent conductivity measurements made using the Geonics EM34-3. Also shown are nearby borehole-based depths to the top of the Triassic, OAG saturated thickness in May 2009, and Triassic depths interpolated from borehole data (dashed line), and noise sources and locations. (bottom) Best-fit conductivity models from time-domain EM soundings (fig. 3; Appendix B) near EM line 3 superimposed on the conductivity pseudosection. Surface elevation from USGS topographic maps and surface elevations, stratigraphic interpretations, contact depths, and water data provided to TCEQ by WCS.

(fig. A3, Appendix A). A parked train interrupted data acquisition and affected EM data quality at about 700 m along the line.

The apparent conductivity pseudosection agrees well with the borehole data (fig. 10). The surface low-conductivity zone increases in thickness northeastward along the line, reflecting the increasing thickness of relatively coarse and dry OAG strata. In the southern part of the FDS along the southern 300 m of the line, near-surface apparent conductivities are high and coincide with shallow depths to conductive Triassic clay-rich strata as well as water-saturated basal OAG strata. Both of these attributes contribute to the observed high near-surface conductivities. Time-domain EM data from this area confirm the elevated near-surface conductivities (W10, fig. 9 and Appendix B) and the approximate depth to the conductive zone representing shallow, clay-rich Triassic strata of the “redbed ridge.”

Line 4

Line 4 was positioned to follow the crest of the postulated “redbed ridge” to examine possible lithologic change along this key subsurface stratigraphic feature (fig. 6). The line begins at the western edge of the FDS and extends 1400 m southeastward across the southern part of the FDS and CDS and a small playa east of the CDS (fig. 3 and table 1). The line ends near the railroad tracks.

The land surface along this line is relatively flat, but the line crosses at least three local lows within the FDS, CDS, and at the playa (fig. 11). Data from 13 boreholes and wells at distances of 4 to 62 m from the line (fig. A4, Appendix A) indicate depths to Triassic strata of less than 10 m along the entire line (fig. 11). Saturated basal OAG strata were reported at well TP-72 near the west end of the line and at wells TP-117 and TP-63 at the playa. Power lines that might affect EM data quality are located near the west and east ends of the line and at a distance of about 700 m along the line. Data acquisition at the 40-m separation did not extend eastward of the playa because of excessive power-line noise (fig. A4, Appendix A).

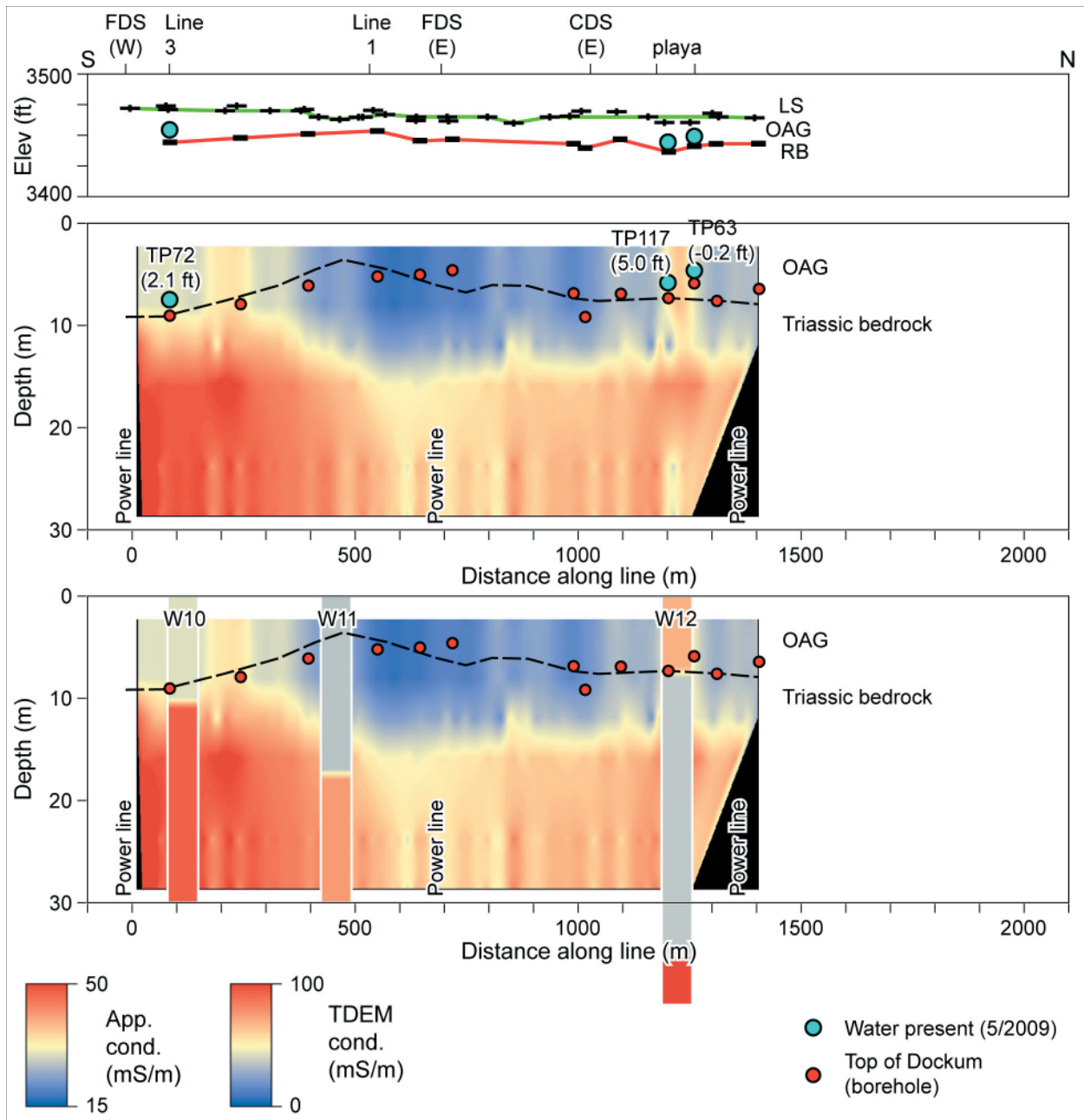


Figure 11. Apparent conductivity pseudosection and supporting data along EM line 4 (fig. 3). (top) Elevation of land-surface (LS) and the top of Triassic redbed surface (RB) and location of wells with OAG water in May 2009. (middle) Gridded apparent conductivity measurements made using the Geonics EM34-3. Also shown are nearby borehole-based depths to the top of the Triassic, OAG saturated thickness in May 2009, and Triassic depths interpolated from borehole data (dashed line), and noise sources and locations. (bottom) Best-fit conductivity models from time-domain EM soundings (fig. 3; Appendix B) near EM line 4 superimposed on the conductivity pseudosection. Surface elevation from USGS topographic maps and surface elevations, stratigraphic interpretations, contact depths, and water data provided to TCEQ by WCS.

The apparent conductivity pseudosection generally depicts a poorly conductive surface layer underlain by a conductive zone. Low, shallow apparent conductivity correlates with borehole-based interpretations of relatively coarse and dry OAG strata from the middle part of the FDS eastward, but the thickness of the poorly conductive zone in this area is about 12 to 15 m, significantly thicker than that based on the top of the Triassic “redbed ridge” as interpreted from borehole data (fig. 11).

Agreement between depths to the conductive layer and depths to Triassic strata is good only at the western end of the line. Beginning at about 400 m along the line, depths to the top of the conductive layer deepen significantly, diverging from borehole-based depths to Triassic strata over an area that includes the eastern half of the FDS and the CDS. EM data suggest that clay-rich, conductive strata along much of this line are significantly deeper than the interpreted top of the Triassic strata. This suggests that either the Triassic stratigraphic pick is correct and that Triassic strata at these shallow depths are coarser-grained (lower clay content) than elsewhere at the site, or that relatively coarse and dry OAG strata are thicker than interpreted from borehole data.

Elevated near-surface apparent conductivity at the western part of the FDS supports the interpretation of shallow, clay-rich Triassic strata and relatively moist OAG strata. Elevated shallow apparent conductivity is also observed at the playa east of the CDS, suggesting an unknown thickness of higher clay content sediments in the playa floor and higher water content associated with playa ponding and downward migration of water.

Line 5

Line 5 begins at the eastern boundary of the LSA pad, extending 1265 m southeastward to the railroad tracks (fig. 3 and table 1). It lies north of the FDS and CDS and the postulated “redbed ridge,” crossing a cluster of wells that reported saturated basal OAG strata in the May 2009 sampling (fig. 6). Stratigraphic and hydrologic information is provided by 9 wells and borings located 0 to 63 m from this line (fig. A5, Appendix A). No major EM noise sources are recognized.

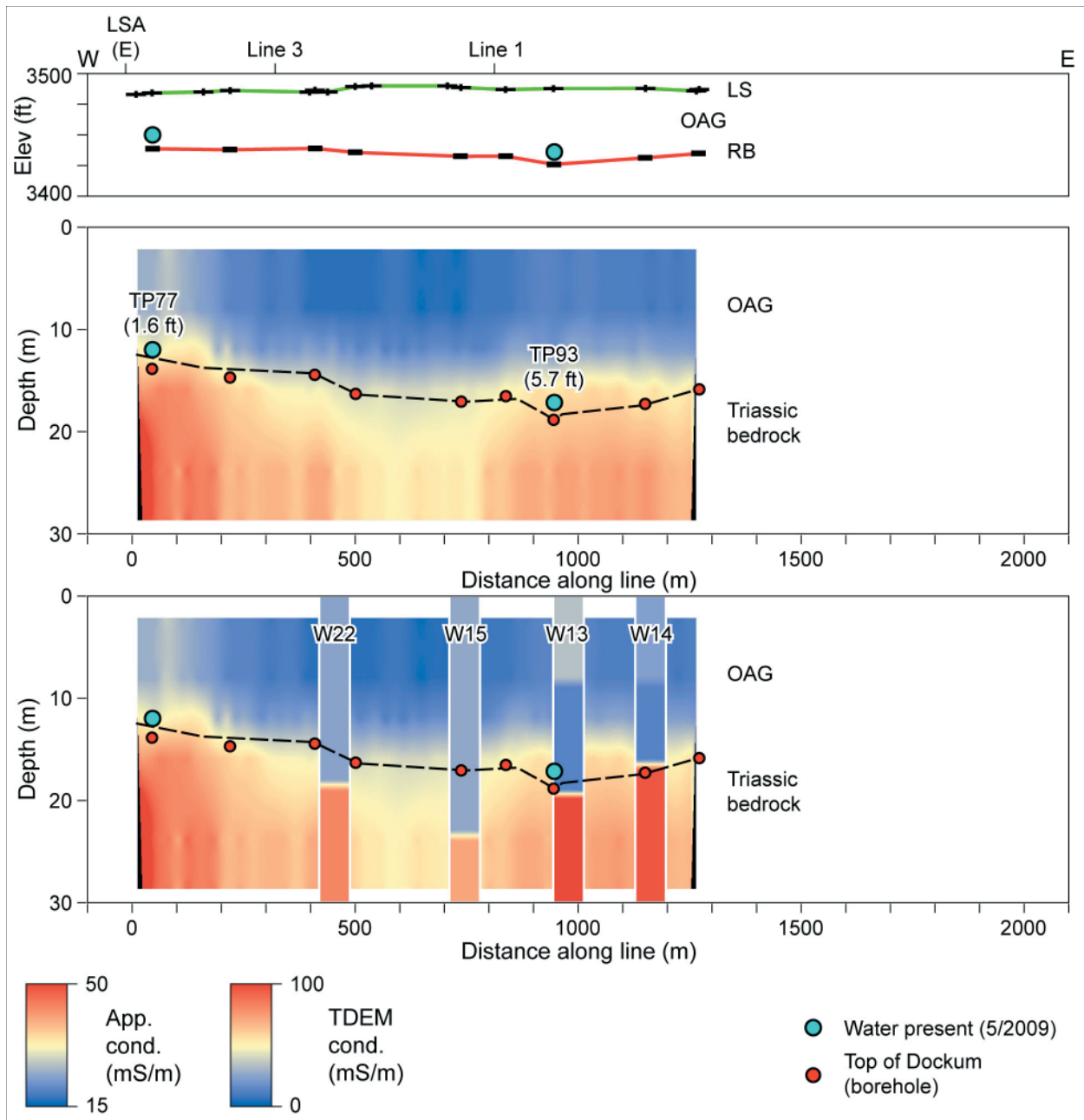


Figure 12. Apparent conductivity pseudosection and supporting data along EM line 5 (fig. 3). (top) Elevation of land-surface (LS) and the top of Triassic redbed surface (RB) and location of wells with OAG water in May 2009. (middle) Gridded apparent conductivity measurements made using the Geonics EM34-3. Also shown are nearby borehole-based depths to the top of the Triassic, OAG saturated thickness in May 2009, and Triassic depths interpolated from borehole data (dashed line), and noise sources and locations. (bottom) Best-fit conductivity models from time-domain EM soundings (fig. 3; Appendix B) near EM line 5 superimposed on the conductivity pseudosection. Surface elevation from USGS topographic maps and surface elevations, stratigraphic interpretations, contact depths, and water data provided to TCEQ by WCS.

Surface topography is relatively flat (fig. 12). Borehole-based OAG thickness generally increases to the southeast along the line, ranging from about 13 to 18 m. Most boreholes are reported to be dry at the base of the OAG, except near the eastern boundary of the LSA pad (0.5 m at TP-77) and at a distance of about 950 m along the line (1.7 m at TP-93) within the cluster of wells having water-saturated basal OAG strata in May 2009 (fig. 3).

The apparent conductivity pseudosection (fig. 12) depicts low apparent conductivity for the interpreted OAG section and higher conductivity within interpreted Triassic rebed strata. Four time-domain EM soundings show basal conductive layer depths that are consistent with those on the pseudosection (fig. 12 and Appendix B). Conductive-layer depths on the pseudosection that are shallower than borehole-based rebed depths are found in the two areas where water-saturated basal OAG strata have been reported: near the LSA pad (0 to 200 m along the line) and within the cluster of water-saturated OAG wells northeast of the FDS (900 to 1100 m along the line), again suggesting that the EM instrument responds to the increase in electrical conductivity that accompanies increased water content in saturated basal OAG strata. Elevated apparent conductivity in the 0 to 10 m depth range at the western end of the pseudosection may indicate increased moisture content within shallower OAG strata near well TP-77 (fig. 12).

The apparent conductivity pseudosection and two of the time-domain EM soundings (W22 and W15, fig. 12 and Appendix B) identify an area (300 to 800 m along the line) where EM data suggest that the basal conductive layer is deeper than the borehole-based top of the Triassic rebeds. This low in the basal conductive zone may reflect a lateral coarsening (lower clay content) in Triassic strata or an underestimated borehole-based OAG thickness in this area.

Differing Triassic and Conductive-Zone Depths

Comparison of apparent conductivity pseudosections with borehole-based stratigraphic interpretations has revealed at least four line segments where depths to interpreted top of Triassic rebeds is significantly shallower than the top of a basal conductive layer interpreted to repre-

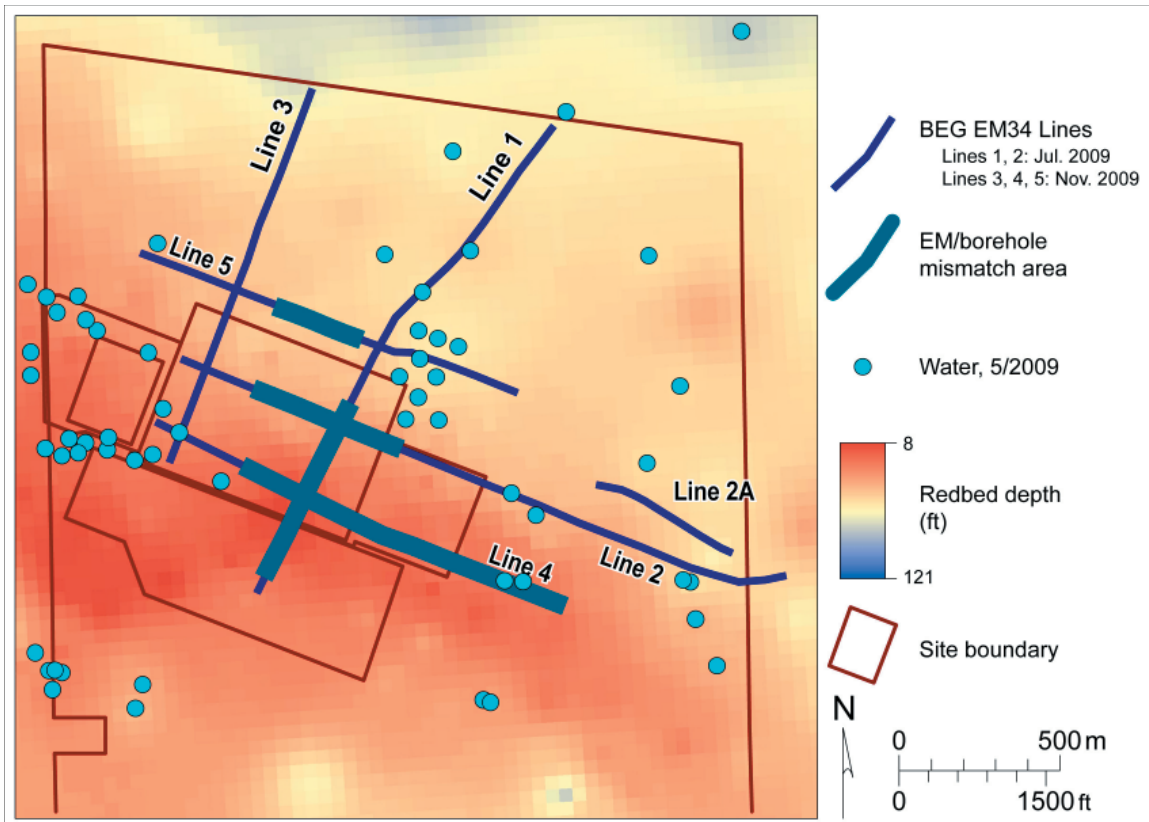


Figure 13. Difference areas (thick blue lines) along EM lines where estimated depths to the electrically conductive layer are significantly deeper than interpreted depths to Triassic redbed strata from boreholes. Also shown are the gridded depth-to-redbed surface and the locations of wells with reported OAG water in May 2009. Borehole data provided by WCS to TCEQ.

sent Triassic clay-rich strata (fig. 13). The depth to the basal conductive zone differs most from borehole-based depths to the top of the Triassic along and across the postulated “redbed ridge.” Along line 1, which crosses the ridge from southwest to northeast, depths to the conductive layer are as much as 11 m greater than borehole-based depths to the top of Triassic strata for a distance of about 550 m from the landfill area across the eastern part of the FDS. Along line 4, which follows the crest of the ridge, depth to the conductive layer is as much as 12 m greater than the borehole-based depth to the top of the Triassic over a distance of more than 1100 m across the southern part of the FDS and CDS (fig. 13). Smaller depth differences are found along a northerly trend that intersects line 2 in the FDS (3 m or less difference over a distance of 500 m) and line 5 north of the FDS (a few meters difference over a distance of about 350 m).

Assuming the EM data accurately represent subsurface electrical properties, it appears likely that these areas where EM data show greater depths to the basal conductive zone are where relatively coarse (lower clay content) strata occupy the depth zone between the borehole-based top of Triassic strata and the EM-based top of the conductive zone. These could be places where a clay-poor Triassic lithologic unit lies beneath low-conductivity OAG strata, or where clay-poor OAG strata are thicker than interpreted from borehole data. In either case, the postulated “redbed ridge” is largely invisible to EM methods, implying that its lithologic composition and perhaps hydrologic properties differ from clay-rich Triassic strata found elsewhere at the site. Lower clay content could suggest greater permeability, which might allow water that would have accumulated at the OAG-Dockum boundary to migrate farther downward to the interpreted clay-rich strata represented by the basal conductive layer.

CONCLUSIONS

Frequency- and time-domain EM measurements appear to have successfully explored to and beyond the base of the OAG section over much of the WCS site. Along most lines, borehole data confirm that dry OAG strata manifest as a poorly conductive surface unit and clay-rich Triassic bedrock manifests as a conductive unit. Pseudosections constructed from frequency-domain EM measurements are most useful for determining the approximate depth to the conductive layer (clay-rich Triassic sediments) and may also help map shallow and deep OAG moisture variations across the site, especially where OAG thickness is well known. Frequency- and time-domain EM data reveal previously undiscovered topography atop the Triassic bedrock as well as places (especially at the “redbed ridge”) where either Triassic lithology changes significantly or bedrock depths from borehole data are underestimated, suggesting that clay-rich strata are significantly deeper than the interpreted bedrock surface beneath parts of the FDS and CDS. EM data also identified shallow OAG strata where elevated conductivity appears to correlate with elevated shallow moisture content or clay and moisture content (playas) that represent potential recharge areas. Elevated conductivities in places above the known bedrock surface may be caused by wa-

ter saturation at the base of the OAG, but would be difficult to verify in the absence of borehole data. Local lows in the basal conductive layer detected along EM lines may indicate areas where OAG water may collect and could guide future monitoring locations.

Perhaps the most significant issue arising from the EM surveys is the possible distinct lithologic nature of the “redbed ridge” beneath the FDS and CDS. There is a large depth discrepancy between stratigraphic picks on the top of the Triassic and the (greater) depth to an electrically conductive layer (clay-rich Triassic strata?) in the general vicinity of the redbed ridge identified in WCS borings. Most future efforts should focus on attempting to better understand the lithologic and hydrologic nature of the ridge and whether it differs from clay-rich Triassic strata encountered elsewhere at the site. Activities could include acquiring and analyzing additional geophysical lines across the eastern end of the ridge especially in the CDS, acquiring new borehole geophysical logs (gamma and conductivity) in selected new boreholes in the areas where a depth discrepancy exists to better characterize the lithology of the zone between the picked base of the OAG and the top of the electrically conductive zone, and moving at least one of the planned fracture test wells farther south in the FDS area to ensure it falls within the area where there is uncertainty about the lithologic composition of the sub-OAG strata. It also seems important to better understand the lithologic, mineralogic, and hydraulic properties of the Triassic strata through sampling and laboratory analysis, particularly contrasting the possible difference between strata within the redbed ridge and more typical Triassic claystone described from borings over much of the site. The main goal of the additional studies would be to better characterize the nature and lateral and vertical extent of the redbed ridge upon which much of the CDS and FDS are situated.

ACKNOWLEDGMENTS

This project was conducted under contract number 582-4-69718 from the Texas Commission on Environmental Quality (TCEQ) to the Bureau of Economic Geology (Bureau). TCEQ staff Conrad Kuharic, Roger Dockery, Gary Smith, and Diane Poteet oversaw project activities and participated in field data acquisition. WCS staff and contractors, including Steve Cook, Gerry

Grisak, Robert Holt, Lynn Yuhr, John Hultman, and Petronila Bustamante, helped coordinate field activities and participated in data collection.

REFERENCES

- Frischknecht, F. C., Labson, V. F., Spies, B. R., and Anderson, W. L., 1991, Profiling using small sources, in Nabighian, M. N., ed., *Electromagnetic methods in applied geophysics—applications*, part A and part B: Tulsa, Society of Exploration Geophysicists, p. 105–270.
- McNeill, J. D., 1980, *Electromagnetic terrain conductivity measurement at low induction numbers*: Mississauga, Ontario, Geonics Limited, Technical Note 6, 15 p.
- Paine, J. G., 2009, *Review of the 2008 resistivity surveys at the WCS Facility, Andrews County, Texas*: Bureau of Economic Geology, The University of Texas at Austin, report prepared for Texas Commission on Environmental Quality, 15 p.
- Parasnis, D. S., 1986, *Principles of applied geophysics*: Chapman and Hall, 402 p.
- Technos, Inc., 2008a *Final Report, Geophysical Survey at the WCS Facility, Andrews County, Texas*: For Waste Control Specialists, LLC, Andrews, Texas, Technos Project No. 08-108, 11 p.
- Technos, Inc., 2008b, *Addendum, Final Report, Geophysical Survey at the WCS Facility, Andrews County, Texas*: For Waste Control Specialists, LLC, Andrews, Texas, Technos Project No. 08-108, 9 p.
- Technos, Inc., 2008c, *Supplemental Report, Additional Resistivity Processing for the Geophysical Survey at the WCS Facility, Andrews County, Texas*: For Waste Control Specialists, LLC, Andrews, Texas, Technos Project No. 08-108, 5 p.
- West, G. F., and Macnae, J. C., 1991, Physics of the electromagnetic induction exploration method, in Nabighian, M. N., ed., *Electromagnetic methods in applied geophysics—applications*, part A and part B: Tulsa, Society of Exploration Geophysicists, p. 5–45.

APPENDIX A: DATA POINTS AND BORINGS
ALONG CONDUCTIVITY PSEUDOSECTIONS

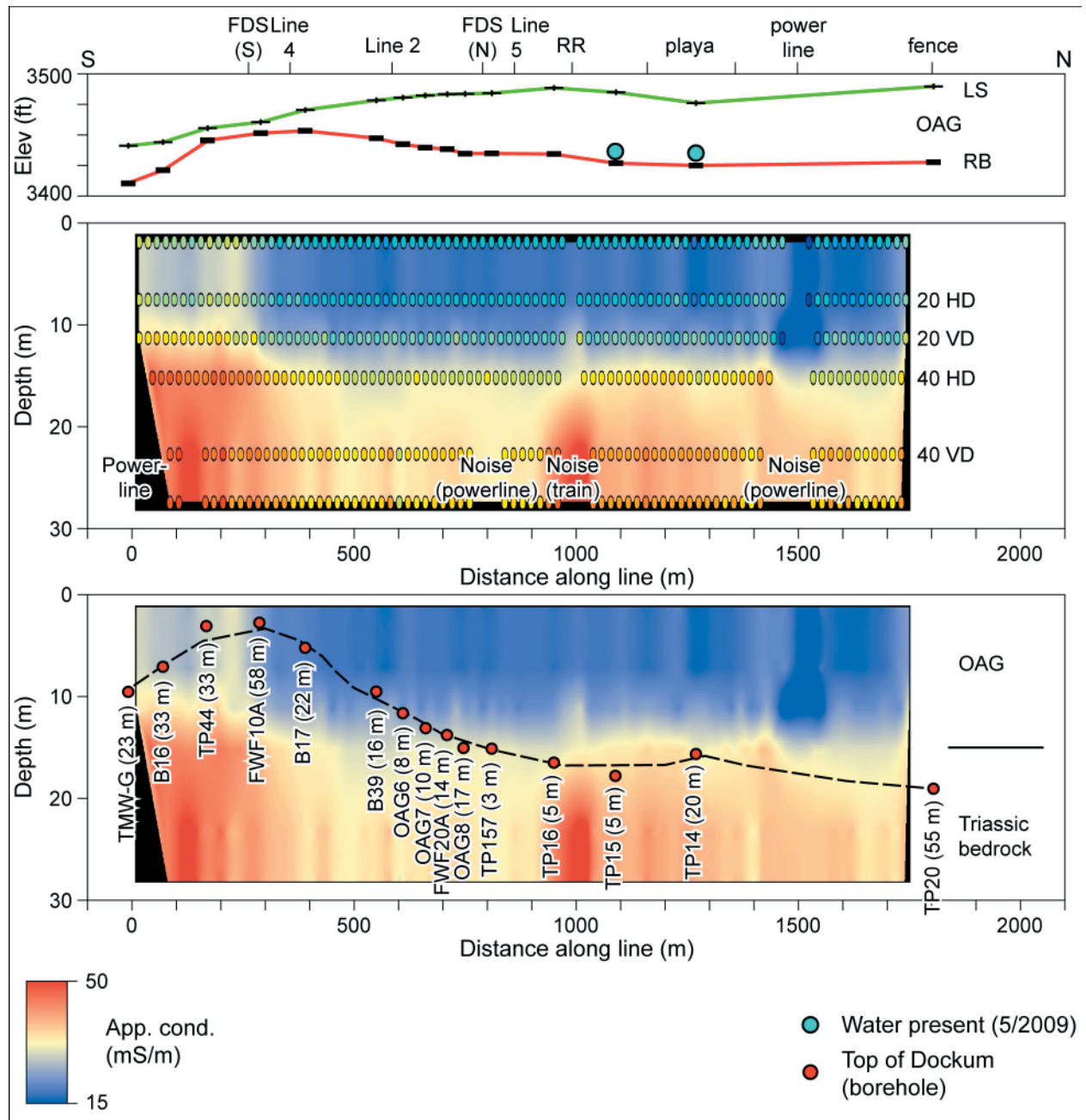


Figure A1. (top) Elevation of land-surface (LS) and the top of Triassic redbed surface and location of wells with OAG water in May 2009 along EM line 1 (fig. 3). Data from USGS topographic maps and elevations and stratigraphic interpretations provided to TCEQ by WCS. (middle) Plotting positions and depths of apparent conductivity measurements made using the Geonics EM34-3 superimposed on gridded apparent conductivity pseudosection. Also shown are noise sources and locations. (lower) Names of borings and wells near EM line 1 with actual and interpolated depths to Triassic redbed strata provided to TCEQ by WCS.

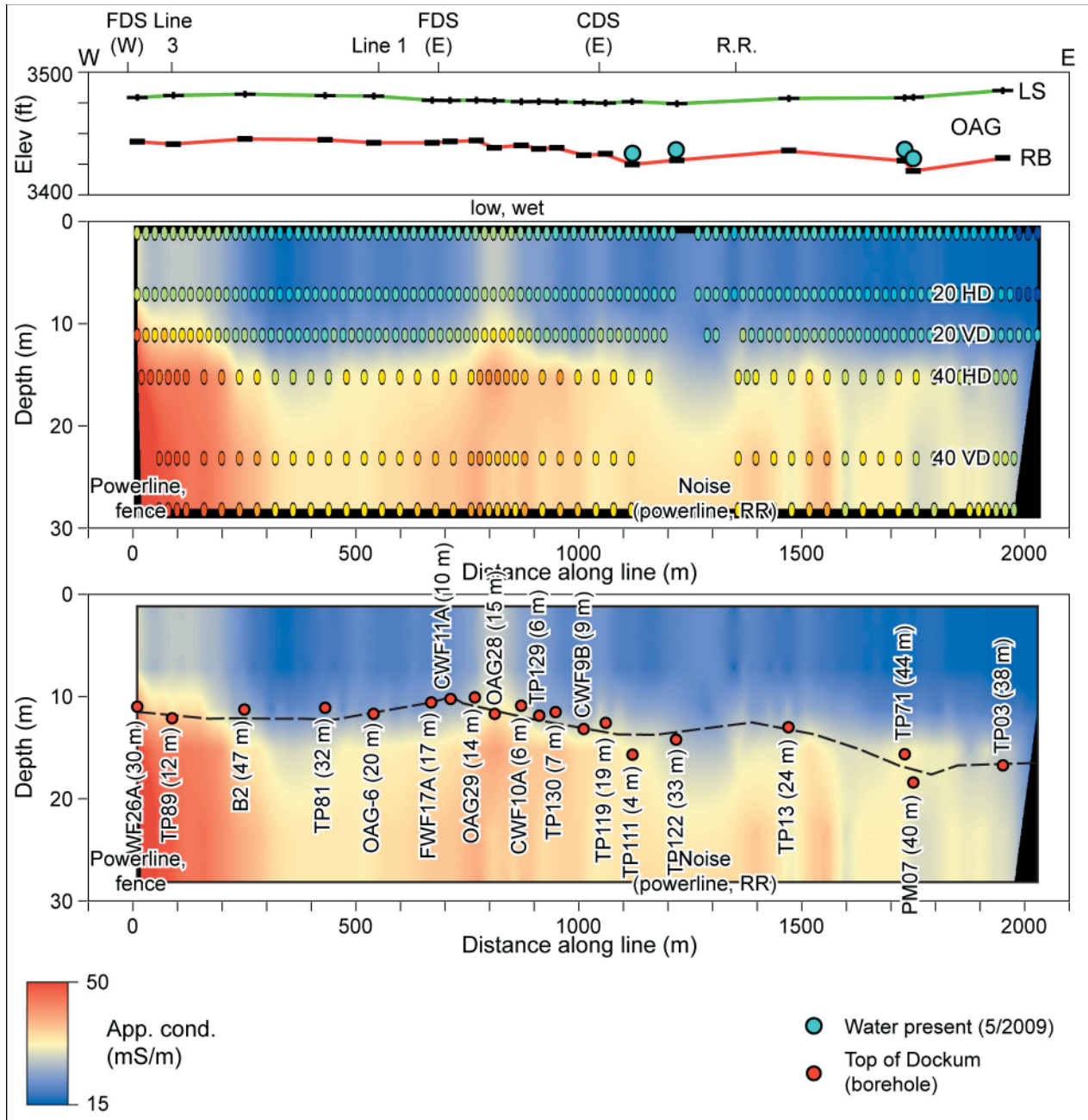


Figure A2. (top) Elevation of land-surface (LS) and the top of Triassic redbed surface and location of wells with OAG water in May 2009 along EM line 2 (fig. 3). Data from USGS topographic maps and elevations and stratigraphic interpretations provided to TCEQ by WCS. (middle) Plotting positions and depths of apparent conductivity measurements made using the Geonics EM34-3 superimposed on gridded apparent conductivity pseudosection. Also shown are noise sources and locations. (lower) Names of borings and wells near EM line 2 with actual and interpolated depths to Triassic redbed strata provided to TCEQ by WCS.

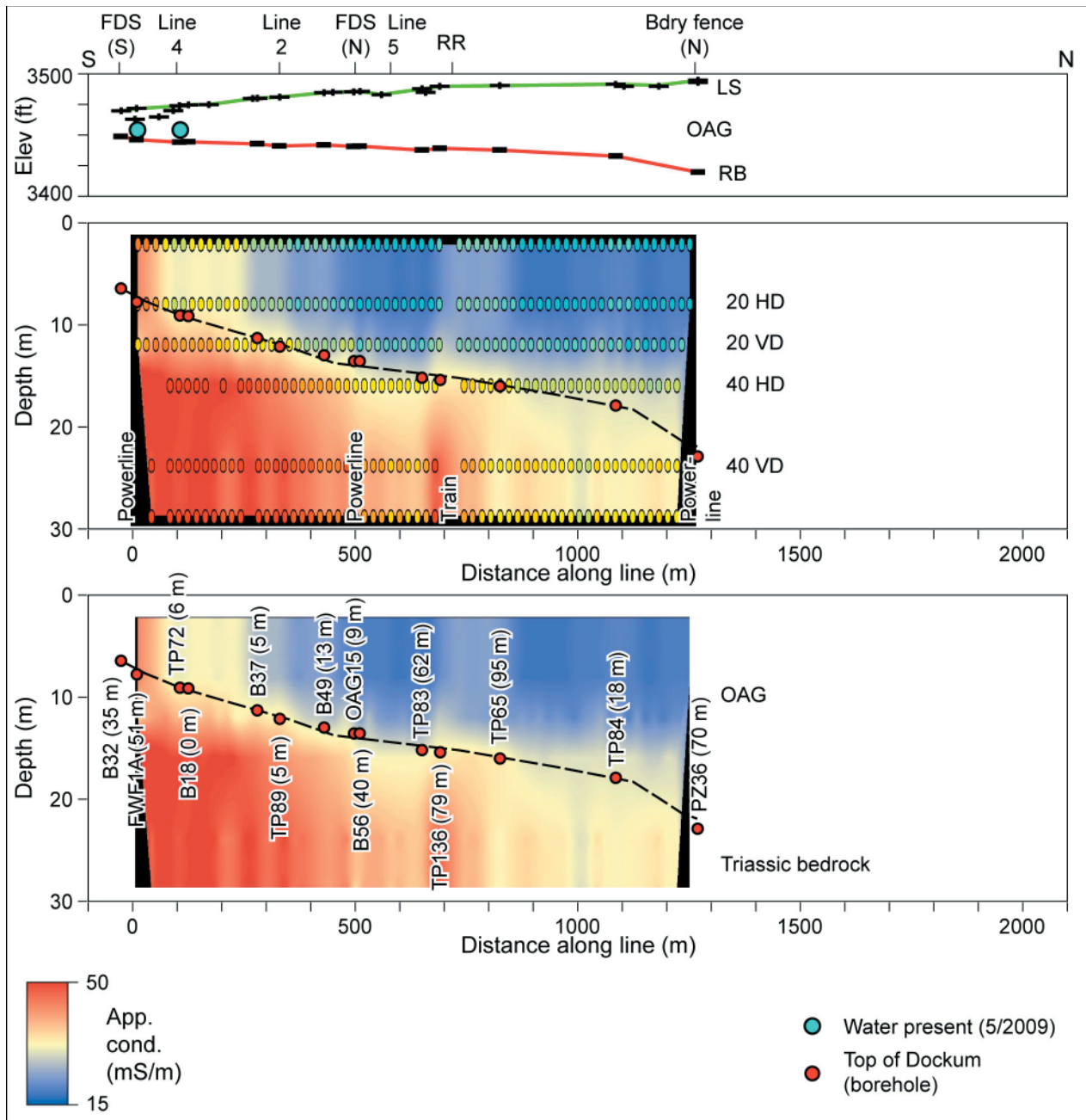


Figure A3. (top) Elevation of land-surface (LS) and the top of Triassic redbed surface and location of wells with OAG water in May 2009 along EM line 3 (fig. 3). Data from USGS topographic maps and elevations and stratigraphic interpretations provided to TCEQ by WCS. (middle) Plotting positions and depths of apparent conductivity measurements made using the Geonics EM34-3 superimposed on gridded apparent conductivity pseudosection. Also shown are noise sources and locations. (lower) Names of borings and wells near EM line 3 with actual and interpolated depths to Triassic redbed strata provided to TCEQ by WCS.

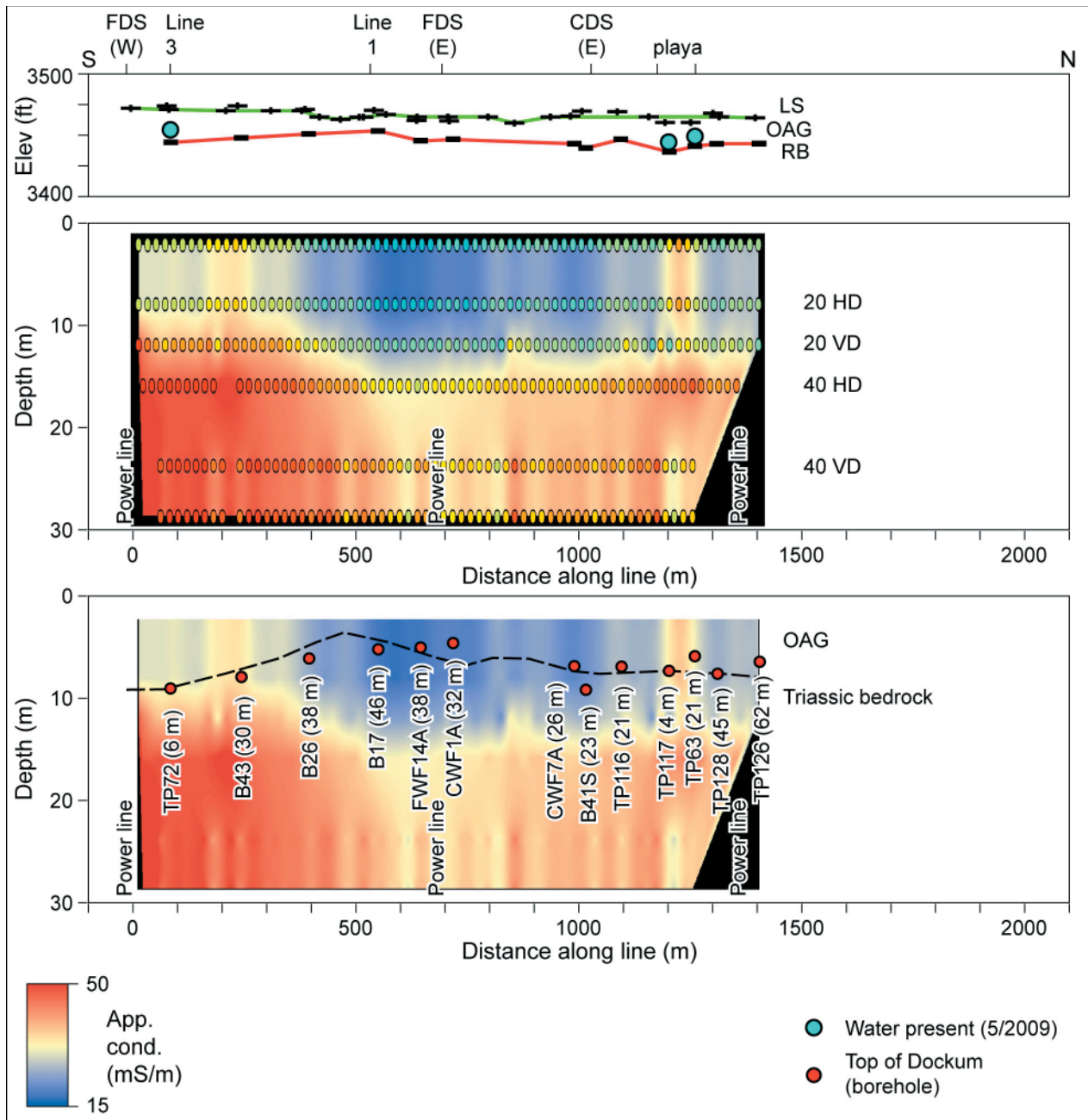


Figure A4. (top) Elevation of land-surface (LS) and the top of Triassic redbed surface and location of wells with OAG water in May 2009 along EM line 4 (fig. 3). Data from USGS topographic maps and elevations and stratigraphic interpretations provided to TCEQ by WCS. (middle) Plotting positions and depths of apparent conductivity measurements made using the Geonics EM34-3 superimposed on gridded apparent conductivity pseudosection. Also shown are noise sources and locations. (lower) Names of borings and wells near EM line 4 with actual and interpolated depths to Triassic redbed strata provided to TCEQ by WCS.

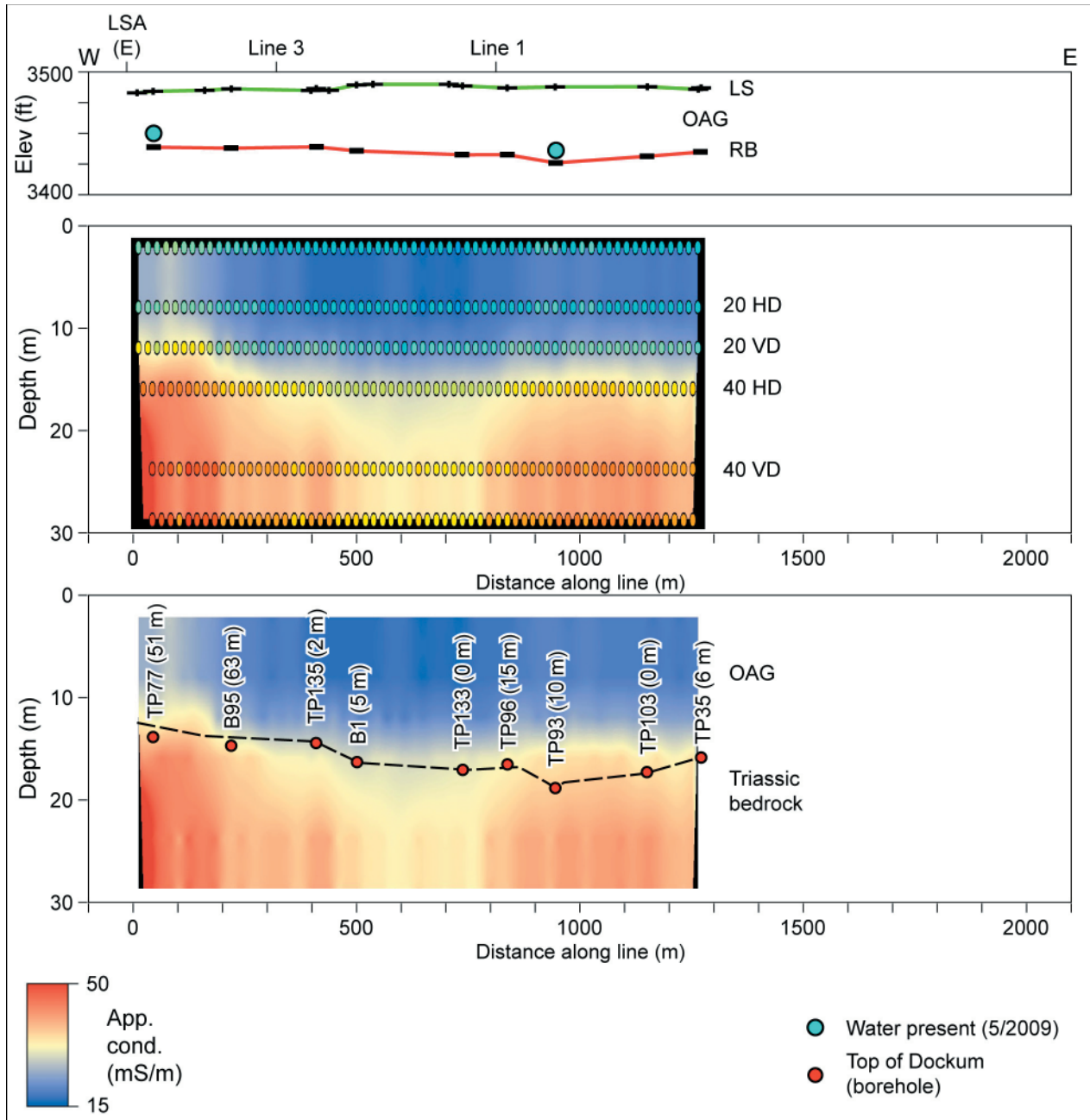


Figure A5. (top) Elevation of land-surface (LS) and the top of Triassic redbed surface and location of wells with OAG water in May 2009 along EM line 5 (fig. 3). Data from USGS topographic maps and elevations and stratigraphic interpretations provided to TCEQ by WCS. (middle) Plotting positions and depths of apparent conductivity measurements made using the Geonics EM34-3 superimposed on gridded apparent conductivity pseudosection. (lower) Names of borings and wells near EM line 5 with actual and interpolated depths to Triassic redbed strata provided to TCEQ by WCS.

APPENDIX B: TIME-DOMAIN ELECTROMAGNETIC INDUCTION SOUNDINGS

Two- or three-layer conductivity models and fitting errors for 14 time-domain EM soundings acquired in November 2009 at the WCS site (fig. 3). Data acquired using a Monex Geoscope terraTEM system, a 20- × 20-m transmitter loop, and a four-turn, 5- × 5-m central receiver loop. Data were processed using the software IX1D v. 3.41 by Interpex.

Sounding	Fitting error (%)	Layer	Conductivity (mS/m)	Resistivity (ohm-m)	Thickness (m)	Depth to top (m)
W10	4.1	1	42.2	23.7	10.6	0
		2	94.1	10.6	-	10.6
W11	3.6	1	34.5	29.0	18.0	0
		2	75.6	13.2	29.5	18.0
		3	127.2	7.9	-	47.4
W12	3.0	1	68.9	14.5	7.7	0
		2	35.8	27.9	28.0	7.7
		3	202.0	5.0	-	35.8
W13	1.4	1	34.0	29.4	8.1	0
		2	12.7	79.0	11.1	8.1
		3	123.9	8.1	-	19.1
W14	3.6	1	22.7	44.0	8.7	0
		2	13.2	75.5	7.7	8.7
		3	95.8	10.4	-	16.4
W15	2.5	1	26.2	38.2	23.6	0
		2	72.6	13.8	36.3	23.6
		3	161.6	6.2	-	59.9
W16	3.3	1	27.5	36.3	20.2	0
		2	98.4	10.2	-	20.2
W17	3.7	1	36.6	27.3	6.4	0
		2	10.4	96.4	10.3	6.4
		3	94.3	10.6	-	16.6
W18	3.4	1	42.1	23.8	14.6	0
		2	15.5	64.4	11.6	14.6
		3	78.5	12.7	-	26.2

W19	3.0	1	41.5	24.1	7.2	0
		2	15.7	63.8	10.0	7.2
		3	67.2	14.9	44.2	17.2
W20	3.6	1	25.6	39.1	17.4	0
		2	72.9	13.7	-	17.4
W21	2.8	1	20.6	48.6	11.2	0
		2	96.5	10.4	-	11.2
W22	4.5	1	24.9	40.2	18.8	0
		2	81.7	12.2	-	18.8
W23	2.2	1	40.4	24.7	12.4	0
		2	75.1	13.3	25.1	12.4
		3	108.0	9.3	-	37.5